Review of Palaeobotany and Palynology 212 (2015) 187–213

Contents lists available at ScienceDirect

Review of Palaeobotany and Palynology

journal homepage: www.elsevier.com/locate/revpalbo

Research paper

Climate-controlled palynofacies and miospore stratigraphy of the Jauf Formation, Lower Devonian, northern Saudi Arabia

Pierre Breuer [a,*], Merrell A. Miller [b], Stanislaw Leszczyński [c], Philippe Steemans [d]

[a] Saudi Aramco, Geological Technical Services Division, Biostratigraphy Group, 31311 Dhahran, Saudi Arabia
[b] IRF Group, Inc., 2357 East 23rd Street, Tulsa, OK 74114, USA
[c] Institute of Geological Sciences, Jagiellonian University, Krakow 31-007, Poland
[d] NFSR Senior Research Associate, Palaeobiogeology, Palaeobotany, Palaeopalynology, Liège University, 4000 Liège, Belgium

ARTICLE INFO

Article history:
Received 16 April 2014
Accepted 14 September 2014
Available online 7 October 2014

Keywords:
Palynofacies
Biostratigraphy
Miospore
Devonian
Saudi Arabia

ABSTRACT

The Jauf Formation miospore succession is synthesized in terms of palaeoenvironments and sequence stratigraphy. The data set for this study is obtained from four overlapping, continuously cored, and extensively sampled, boreholes that form a 940 ft (287 m) composite section. The Jauf Formation ranges in age from late Pragian to latest Emsian. The palynological assemblages, recognized herein, provide the basis for recognizing depositional environments present in the Lower Devonian of northern Saudi Arabia. Transgressive–regressive cycles are indicated not only by lithology, but also by marked changes in the marine to terrestrially dominated palynological assemblages, which are described in detail. Flooding events are recognized by the replacement of spore-dominated assemblages by organic-walled microphytoplankton and could be climate-controlled. The maximum flooding interval for the Jauf Formation is reinterpreted based on a correlative event consisting of diverse acritarchs and abundant chitinozoans. The sequence of palynological assemblages corresponds to fourth order cycles in the Hammamiyat Member. The new northern Gondwanan biozonation developed by Breuer and Steemans (2013) and used here allows a high-resolution regional biozonation for the Arabian Plate and larger-scale correlation of the Jauf Formation with other Gondwanan and Euramerican localities. One new spore genus (*Zonohilates*) and four new spore species (*Insculptospora maxima*, *Camarozonotriletes alruwailii*, *Devonomonoletes crassus* and *Zonohilates vulneratus*) are proposed.

1. Introduction

Dispersed plant spores are the primary tool used for biostratigraphic age determination and correlation of the Devonian deposits of Saudi Arabia supplementing marine faunas that are confined to Jauf Formation outcrops (e.g. Boucot et al., 1989; Forey et al., 1992). More than a decade ago, Saudi Aramco drilled a number of shallow core holes in northern Saudi Arabia with the intention of studying the Devonian deposits of this area and correlating them to the nearby outcrops. Leszczyński et al. (2010) described the sedimentology of two pairs of core holes located ca. 350 km apart (Fig. 1), and documented the bioturbation and sedimentological structures present in the Jauf Formation (Figs. 2 and 3). The JNDL-3 and JNDL-4 core holes are located in the vicinity of Domat Al-Jandal while BAQA-1 and BAQA-2 are near the town of Baq'a. The Jauf Formation in northern Saudi Arabia is divided into five members based on lithofacies. The lower part of formation occurs in the BAQA core holes whereas its upper part occurs in JNDL-3 and JNDL-4. Stratigraphic overlap of the cores gives a complete composite Jauf Formation succession (942 ft/287 m thick) and includes all members (Fig. 4).

These core holes were studied palynologically to establish a detailed Devonian biostratigraphy and correlate with subsurface sections from eastern Saudi Arabia (Breuer et al., 2005, 2007; Breuer and Steemans, 2013). Palynological slides from previous studies were re-examined and complemented by newly processed samples and observations. This paper represents the synthesis for the spore-based stratigraphy of the Jauf Formation in northern Saudi Arabia. Although the majority of spore species from the studied assemblages were described by Breuer et al. (2007) and Breuer and Steemans (2013), some are new and described below in the Systematic Palaeontology. Finally the results of the quantitative study carried out on palynological assemblages are presented herein and palaeoenvironments are discussed regarding the detailed sedimentological study of the sections by Leszczyński et al. (2010).

2. Jauf Formation

The Jauf Formation is exposed in northern Saudi Arabia (Powers, 1968). The formation is described in the explanatory notes of several geological quadrangle maps where it is present (Vaslet et al., 1987;

* Corresponding author. Tel.: +966 13 873 0302; fax: +966 13 873 1009.
E-mail address: pierre.breuer@aramco.com (P. Breuer).

http://dx.doi.org/10.1016/j.revpalbo.2014.09.005
0034-6667/

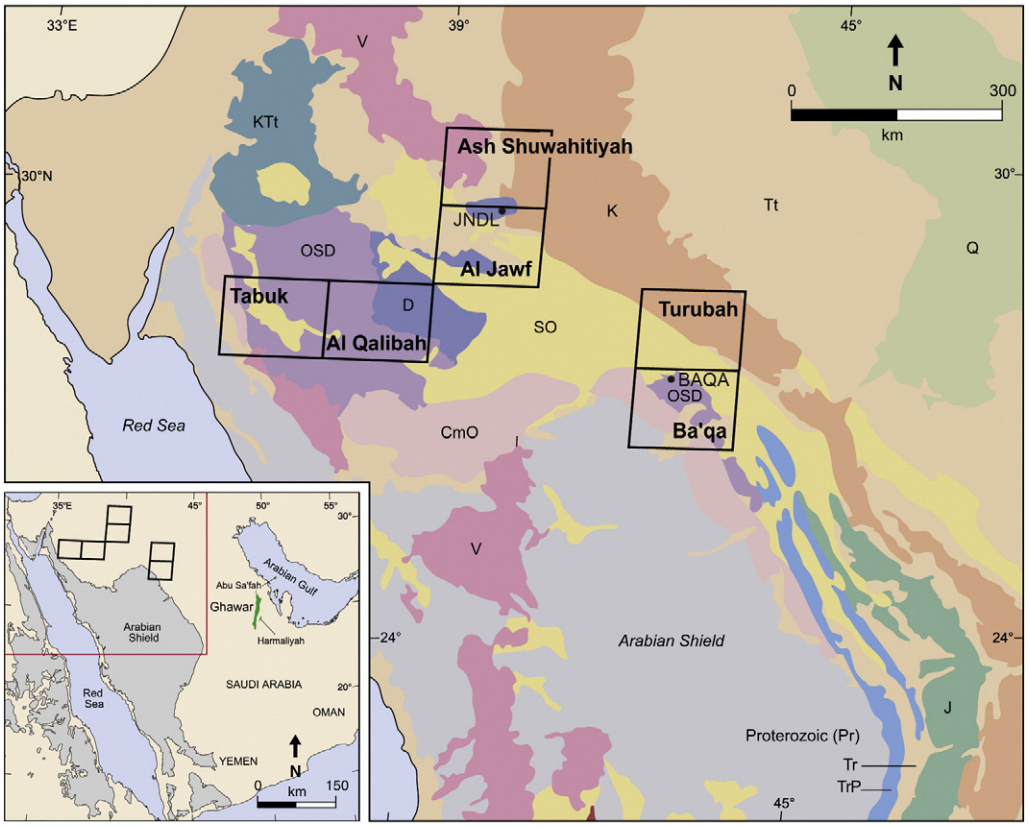

Fig. 1. Location of core holes discussed in this study. The Jauf Formation exposed in northwestern Saudi Arabia was described from indicated geological quadrangles (Devonian indicated by the letter D; undifferentiated Ordovician–Silurian–Devonian indicated as OSD).

Wallace et al., 1996, 1997; Janjou et al., 1997a,b; Lebret et al., 1999). The Jauf Formation in outcrop was also studied by Helal (1965), Bahafzallah et al. (1981), Al-Laboun (1982, 1986) and Al-Husseini and Matthews (2006). Macrofauna from the Jauf Formation were investigated for brachiopods (Boucot et al., 1989) and fish (Forey et al., 1992). Spore assemblages were only recorded from the subsurface (see below). Over many Arabian Plate tectonic structures and palaeohighlands the Jauf formation is absent because of Late Palaeozoic uplift and subsequent erosion (Wender et al., 1998; Konert et al., 2001). In eastern Saudi Arabia, the Jauf Formation is only present in the subsurface (e.g. Wender et al., 1998; Al-Hajri et al., 1999).

In northwestern Saudi Arabia, the Jauf Formation varies in measured thickness between 886 ft (270 m) and 1083 ft (330 m) (Helal, 1965; Powers, 1968; Boucot et al., 1989; Wallace et al., 1997). It overlies disconformably or unconformably the continental to shallow-marine Tawil Formation, and is unconformably overlain by the continental Jubah Formation. Although the shift from continental (Tawil) to marine (Jauf) sedimentation would presumably involve a hiatus, some authors interpret the Jauf/Tawil Formation contact to be conformable (e.g., Powers, 1968; Vaslet et al., 1987; Al-Hajri et al., 1999). Others declare that the Jauf Formation overlies the Tawil Formation in disconformity (Janjou et al., 1997a; Wallace et al., 1997) or unconformity (Wallace et al., 1996). Although the contact between the Jauf and Jubah Formations appears to be conformable (Al-Hajri et al., 1999), the upper part of the Jauf Formation (Murayr Member) is unconformably overlain by Jubah sandstone beds (Wallace et al., 1996, 1997; Janjou et al., 1997a). This major erosional boundary between the Murayr tidal sandstone and the Jubah fluvial sandstone reflects an abrupt change in the sedimentary environment and is a sequence boundary.

2.1. Lithostratigraphy

The alternating siliciclastics and carbonates of the Jauf Formation in northwestern Saudi Arabia are used to subdivide it into five members: the Sha'iba, Qasr, Subbat, Hammamiyat and Murayr members (in ascending order). The five members constitute a conformable succession according to Wallace et al. (1996, 1997). Although the lithological characters of the Jauf Formation change little throughout northwestern Saudi Arabia, the different members are described according to the region where the studied core holes cut through them (Figs. 2 and 3).

2.1.1. Sha'iba Member

This unit is only drilled by BAQA-2 core hole (Fig. 2). In the Baq'a Quadrangle (Vaslet et al., 1987), the Sha'iba Member in outcrop is composed in the lower part of beige fine-grained sandstone sometimes with cross-bedding and reworked clay galls and plant remains. This sandstone interval is capped by a ferruginous surface. The interval above comprises green to red, micaceous silty claystone including rare pinkish, laminated, silty dolomite at the base. The 6.5 uppermost feet (2 m) are composed of yellow to pinkish, lenticular dolomite intercalated with ochre, laminated, fine-grained sandstone and green, micaceous, silty claystone. Estimate of the thickness inside the Baq'a Quadrangle in the Al Muyyah section is 85 ft (26 m) (Vaslet et al., 1987) whereas the Sha'iba Member is about 121 ft (37 m) thick in BAQA-2 (Fig. 2). In the Baq'a Quadrangle, the contact between the Jauf and the underlying Tawil Formations is sharp and characterized by a reworking of the palaeosol capping the Tawil sandstone and is conformable according to Vaslet et al. (1987). This boundary is distinctively marked by plant root structures in BAQA-2 (Fig. 2).

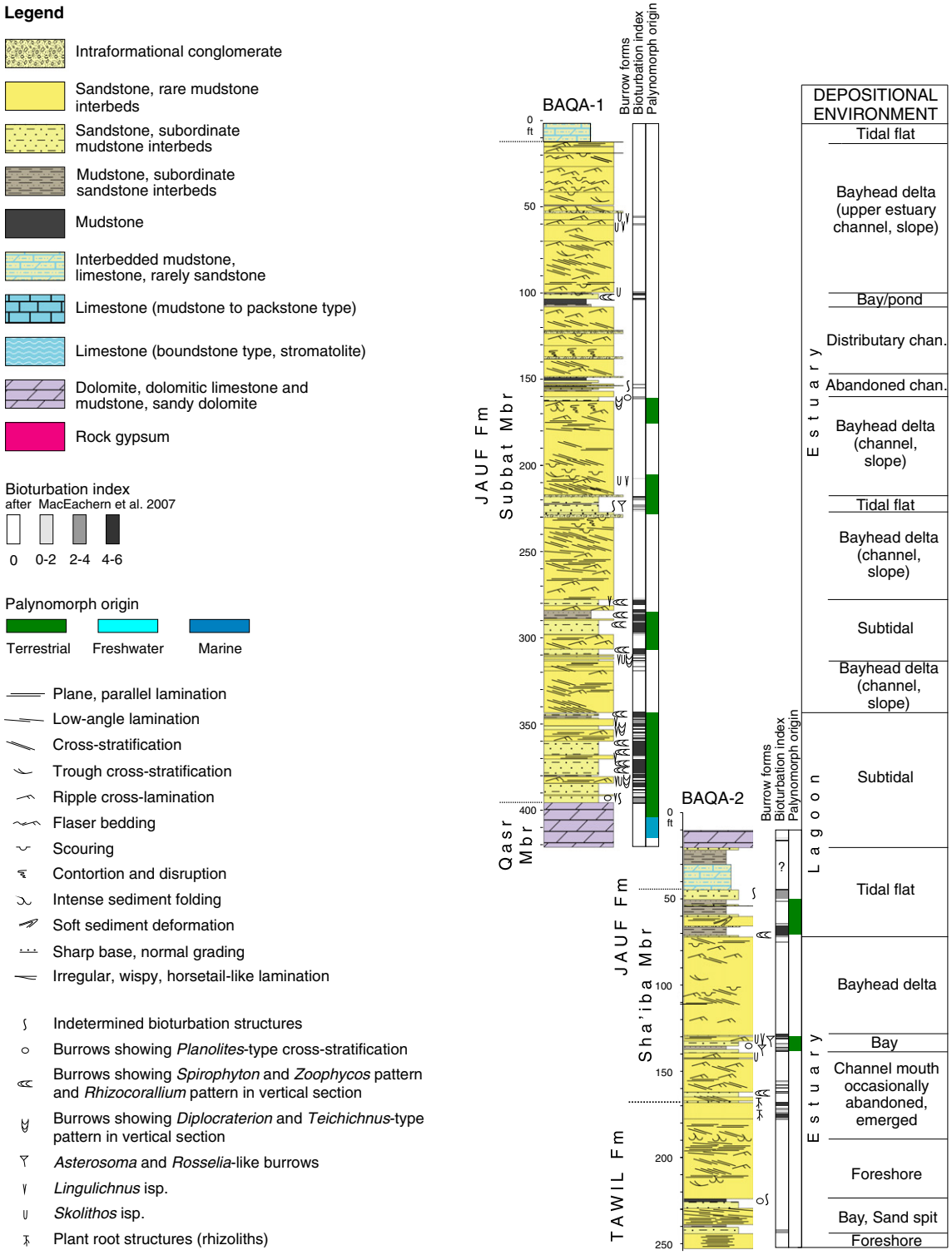

Fig. 2. Generalized core logs from the BAQA core holes, showing main rock types, sedimentary structures, ichnology, intensity of bioturbation structures, intensity of bioturbation, environmental origin of palynomorph assemblages and inferred depositional environments (modified after Leszczyński et al., 2010).

2.1.2. Qasr Member

This unit is drilled by BAQA-1 and BAQA-2 core holes (Fig. 2). In the Baq'a Quadrangle (Vaslet et al., 1987), the Qasr Member in outcrop is composed, in the lower part, of beige to gray, oolitic and stromatolitic dolomite with reworked clay galls at the base. The stromatolites show a columnar pattern. The overlying interval is brown, micaceous, clayey siltstone of 13 ft (4 m) in thickness. The uppermost 20 ft (6 m) comprises gray to yellowish, sparitized dolomite. Massive benches of very bioclastic facies with oolites at the top and more laminated facies near the base occur. Estimate of the thickness inside the Baq'a Quadrangle in the Al Muyyah section is 46 ft (14 m) (Vaslet et al., 1987) as measured in BAQA-2 (Fig. 2).

2.1.3. Subbat Member

This unit is drilled by BAQA-1 core hole (Fig. 2) in the Baq'a Quadrangle and by JNDL-4 (Fig. 3) in the Al-Jawf Quadrangle. In the Baq'a

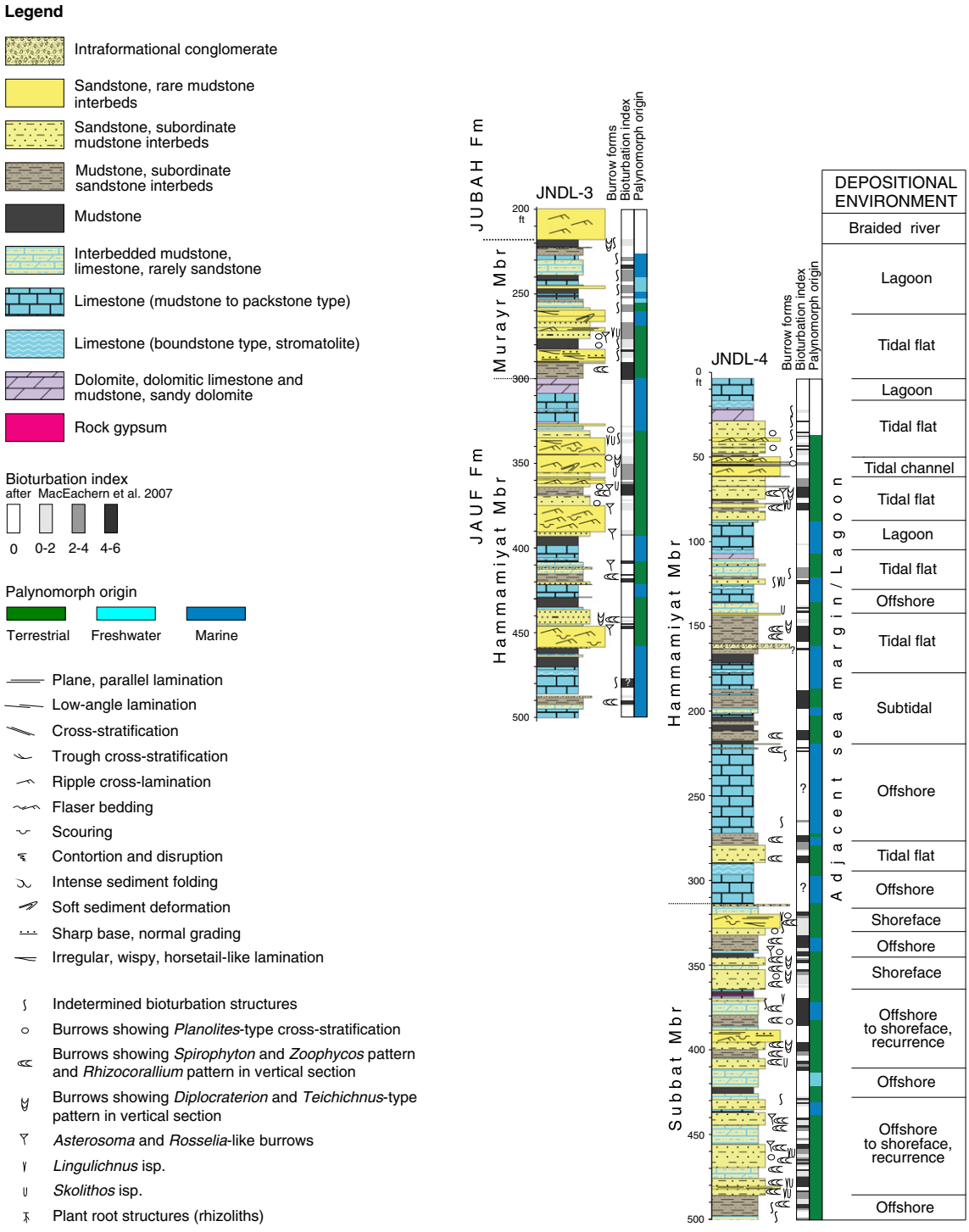

Fig. 3. Generalized core logs from the JNDL core holes, showing main rock types, sedimentary structures, ichnology, intensity of bioturbation structures, intensity of bioturbation, environmental origin of palynomorph assemblages and inferred depositional environments (modified after Leszczyński et al., 2010).

Quadrangle (Vaslet et al., 1987), the Subbat Member in outcrop is mainly composed of gray or white, fine-grained, commonly cross-bedded or laminated sandstone, intercalated with greenish silty claystone. In the lower part, a decimetre-sized layer of sub-bituminous coal occurs with abundant plant remains. The Subbat Member in JNDL-4 is more shale-dominated (Fig. 3) but more sand-dominated in BAQA-1 (Fig. 2). In the Al-Jawf Quadrangle (Wallace et al., 1997), the Subbat Member in outcrop is variegated shale that contains detrital mica on bedding surfaces. The shale is silty with common secondary gypsum veins. Interbedded grayish-red, gray, and reddish-gray sandstone beds range from several centimetres to 6.5 ft (2 m) in thickness. A prominent reddish-tan-weathering, ripple-marked sandstone, about 6.5 ft (2 m) thick, is present near the top of the member that is also recognized in JNDL-4 (Fig. 3). Estimates of the thickness are 328 ft (100 m) (Helal, 1965; Vaslet et al., 1987), 372 ft (113.4 m) (Powers, 1968), or about 371 ft (113 m) (Boucot et al., 1989). The thickness of the Subbat Member in BAQA-1 is about 382 ft (116 m) (Fig. 2) but cannot be determined in JNDL-4 because the base is not reached (Fig. 3).

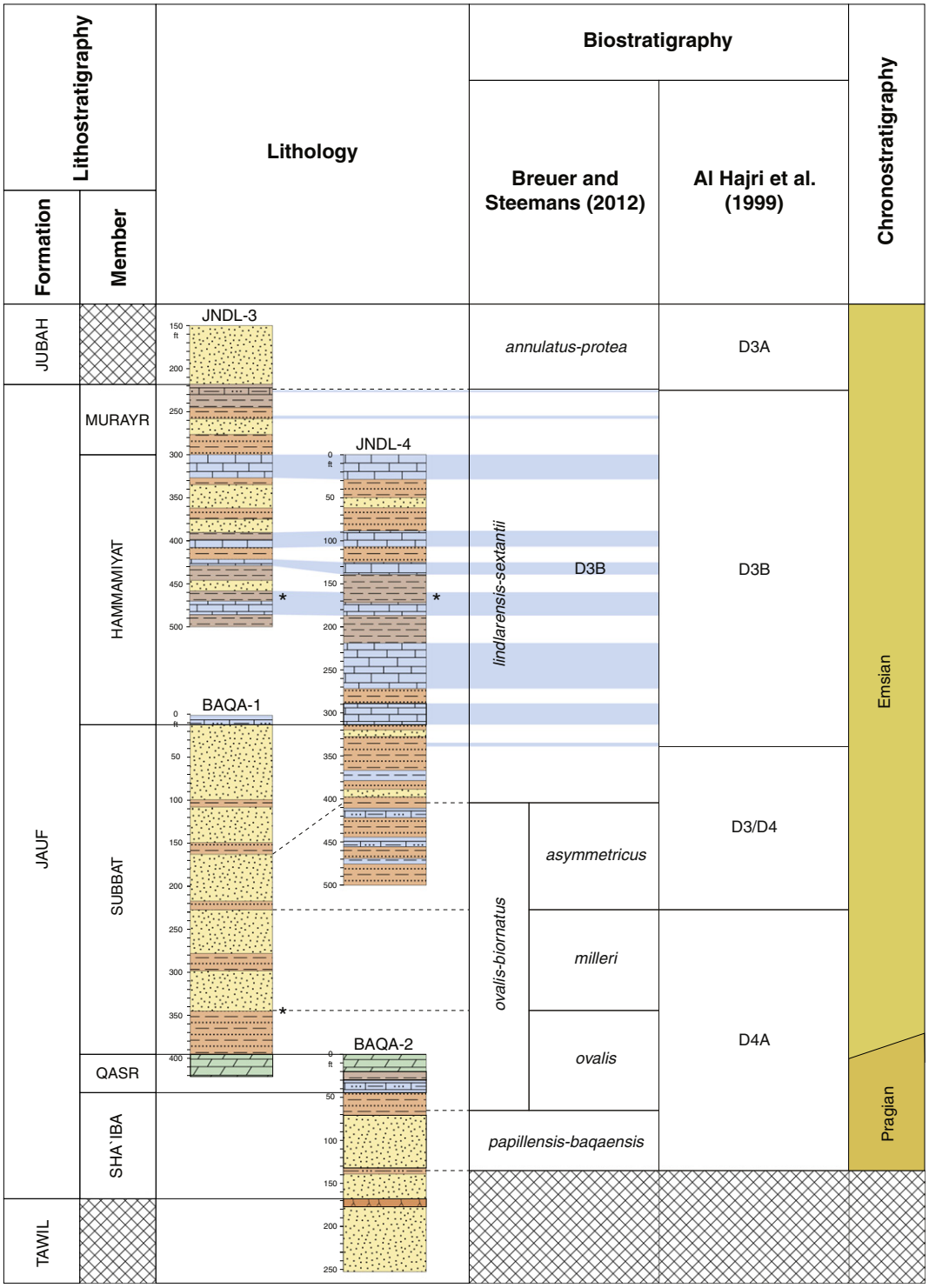

Fig. 4. Lithostratigraphy, lithology, biostratigraphy and chronostratigraphy for a composite section of the Jauf Formation core holes (*chitinozoan occurrence).

2.1.4. Hammamiyat Member

This unit is penetrated by JNDL-3 and JNDL-4 core holes (Fig. 3). In the Al-Jawf Quadrangle, the Hammamiyat Member according to (Wallace et al., 1997) is an interval of moderate gray-, tan-, or light-grayish-yellow-weathering, stromatolitic, finely crystalline limestone interbedded with shale. Helal (1965) and Boucot et al. (1989) described six limestone zones that range from 13–36 ft (4–11 m) in thickness, which are separated by light-gray, grayish-brown, and yellowish-brown shale and rare beds of gray, fine-grained sandstone. They can be recognized in the studied sections (Fig. 3). Stromatolites are as much as one metre in diameter and occur as laterally linked hemispheroids and as isolated heads that are 10–20 cm in diameter. Shale beds contain primary gypsum in thin layers and secondary gypsum fills fractures and joints. Estimates of the thickness in the Al-Jawf Quadrangle are 387 ft (118 m) (Helal, 1965; Wallace et al., 1997), 349 ft (106.3 m) (Powers, 1968) or 344 ft (105 m) (Boucot et al., 1989). The measured thickness of the Hammamiyat Member in JNDL-4, where it is complete, is 312 ft (95 m) (Fig. 3).

2.1.5. Murayr Member

This unit is only present in the JNDL-3 core hole (Fig. 3). The Murayr Member was previously named the 'transition zone member' (Powers, 1968) or the informal Fiy'adh Member (Al-Hajri et al., 1999). In the Al-Jawf Quadrangle (Wallace et al., 1997), the Murayr Member, in outcrop, is a light gray and light-grayish-brown sandstone that weathers to reddish-brown and grayish brown. Sandstone, siltstone and shale beds are poorly indurated. The sandstone is thinly bedded (2–8 cm), and contains ripple cross-lamination, planar lamination, rib-and-furrow structure, and small- to medium-scale crossbeds. The sandstone beds generally coarsen upward and are mostly medium-grained at the base becoming fine-grained in the upper part of the member; most grains are subangular and subrounded. The sandstone is micaceous and some beds contain fragmentary fish bones. The shale and siltstone are light green to light tan, and these fine-grained rocks contain abundant secondary gypsum and one thin bed of chert. A gastropod coquina bed near the top of this unit was first described by Lozej (1983), and although only 2–3 cm thick, it is an easily recognizable marker bed near the top of the Murayr Member. The Murayr Member is 108 ft (33 m) thick to the north of Domat Al-Jandal but thins near this locality. Indeed, the unit is 82 ft (25 m) thick in JNDL-3 (Fig. 3).

2.2. Depositional environments and sequence stratigraphy

2.2.1. Sha'iba Member

The basal part of the Sha'iba Member was deposited in a transgressive, shallow-marine and nearshore setting over low local topography (Boucot et al., 1989). This environment succeeded, fairly abruptly, the sand-dominated, tidally influenced deltaic system of the upper part of the Tawil Formation. In Baq'a Quadrangle, the Sha'iba Member is sand-dominated. In BAQA-2, it was deposited in a bay-type environment in which sandstone bodies accumulated either at the mouths of tidal distributary channels, or as tidal flats in the upper part (Fig. 2).

2.2.2. Qasr Member

The clastic beds in the Qasr Member were interpreted to have been deposited in deeper water than those of the underlying Sha'iba Member (Boucot et al., 1989). Stromatolitic and oncolitic limestone beds represent deposition in a shallow-marine, subtidal environment within the photic zone. Beds containing fish remains may record brackish-water estuarine conditions (Boucot et al., 1989). Janjou et al. (1997a) interpreted the sediments of the Qasr Member to represent a carbonate-rich lagoonal environment in which argillaceous sediments were succeeded by stromatolitic carbonates characteristic of an environment relatively free of terrigenous sediment input. The progressive reduction in the influx of terrigenous material toward the top of the member may reflect a relative rise in sea level and led to the deposition of the stromatolitic carbonates.

2.2.3. Subbat Member

The lowermost part of the Subbat Member is interpreted to be deposited in a siliciclastic lagoonal system of principally argillaceous sedimentation succeeded by meandering channels, and characterized by low energy subtidal influence (Fig. 2). Progradation of this terrigenous lagoon sequence over the marine carbonates of the Qasr Member represents a regressive phase that succeeded the first transgressive episode at the base of the Jauf Formation. The remainder of the Subbat is deposited in an estuary system in BAQA-2 (Fig. 2). In many places in the Baq'a Quadrangle, the uppermost parts of the Subbat Member are incised by large-scale, fluvial-dominated valleys, which are filled with red to light brown, large-scale cross-bedded, coarse- to very fine-grained, fining-upward sandstones. They may be more than 49 ft (15 m) thick and 164 ft (50 m) wide. Their erosional bases represent sequence boundaries as a result of substantial fall in sea level. All the evidence suggests that the Subbat Member was deposited in a transgressive systems tract. In JNDL-4 which is more shale-dominated, the depositional environment of the Subbat Member is interpreted to be shallow-marine and nearshore in a region of low relief (Fig. 3); in most respects, it was deposited in an environment similar to the Sha'iba Member (Boucot et al., 1989).

2.2.4. Hammamiyat Member

According to Boucot et al. (1989), the general depositional environment of the Hammamiyat Member was shallow-marine and distant from shore and sources of clastic debris; muds and rare sand bars accumulated in quiet water below wave base. JNDL-4 and JNDL-3 core holes show a great variety of depositional environments from carbonate offshore to siliclastic tidal complexes (Fig. 3). According to Al-Husseini and Matthews (2006), the Hammamiyat Member is subdivided into six units, which correspond to the six T–R cycles previously identified by Janjou et al. (1997a). As pointed out by Al-Husseini and Matthews (2006), the two lower units are principally carbonate and indicate maximum distance from the terrigenous source. The base of the final unit 6 indicates a high energy hydrodynamic system and the presence of increasing terrigenous input, followed by a return to carbonate sedimentation (Fig. 3).

2.2.5. Murayr Member

The Murayr Member was deposited in a brackish and estuarine environment and the sandstone beds may represent beach deposits and estuarine channels (Boucot et al., 1989). The lower part of the Murayr Member in JNDL-3 was deposited in a tidal flat environment. The thin carbonate beds in the upper part highlight high frequency transgressive fluctuations that replaced estuarine sedimentation by more-lagoonal deposition (Fig. 3). The sediments of the Murayr Member were deposited by a regressive siliciclastic estuarine complex (Janjou et al., 1997a), which was the harbinger of deposition of the mostly continental Jubah Formation.

In contrast to the sandstones of the underlying Tawil and overlying Jubah Formations, the limestones of the Jauf Formation clearly reflect an open-marine depositional environment in northwestern Saudi Arabia. The Jauf Formation, however, changes from marine influenced in northwestern Saudi Arabia to marginal marine/continental in central and southern regions (Al-Hajri et al., 1999; Al-Hajri and Owens, 2000). In the subsurface of eastern Saudi Arabia, Rahmani et al. (2002) divided the Jauf Formation into a lower member or Sequence S1 and middle and upper members both forming Sequence S2. The D3B Palynosubzone (Al-Hajri et al., 1999) occurs in a mainly dark-colored marker shale at the top of the transgressive system tract of Sequence S2 (Rahmani et al., 2002). Wender et al. (1998) suggested a similar interpretation in which the D3B Palynosubzone was considered as a possible condensed section and maximum flooding interval. Rahmani et al. (2002) interpreted each of the two sequences of the Jauf Formation as third-order. They identified 16 fourth-order sequences in Sequence S1 and 15 in Sequence S2. Sequence S1 is probably correlative with the Sha'iba, Qasr and lower Subbat members. Sequence S2 may be equivalent to the Hammamiyat and Murayr members. Rahmani (2004) described Sequence S1 as dominated by a falling stage systems tract (forced regressive shoreface), which prograded from west to east over a distance of 150–200 km. Sequence S2 comprises transgressive and highstand system tracts.

Al-Husseini and Matthews (2006) demonstrated that the deposition of the Jauf Formation in outcrop (from the Al Qalibah Quadrangle) corresponds to a second-order transgressive–regressive cycle and manifests several stratigraphic elements that can be interpreted in terms of third- and fourth-order orbital cycles. Al-Husseini and Matthews (2005) calibrated a periodic second-order sequence stratigraphic framework for the Arabian Phanerozoic succession on the basis of a simplified orbital-forcing model of sea-level. In this framework, each second-order depositional sequence (denoted DS^2) was deposited during a constant period of approximately 14.58 million years (my). The Jauf Formation corresponds to the 28th sequence (DS^2 28) and was deposited between second-order sequence boundaries (denoted SB^2) that

coincide with the Jauf/Tawil Formation boundary (SB2 28 at 407.6 my) and Jubah/Jauf Formation boundary (SB^2 27 at 393.0 my). The second-order cycle can be characterized in terms of an initial flood (Qasr Member), followed by a more regional flood (Hammamiyat Member). The Hammamiyat flood can be recognized across Saudi Arabia thanks to the presence of the D3B Palynosubzone (Al-Hajri et al., 1999). The six units of the Hammamiyat Member appear to be fourth-order cycles and could constitute a third-order deposition sequence according to Al-Husseini and Matthews (2006). The lower units 1 and 2, which are principally carbonate, represent maximum transgression in the Jauf Formation. The upper units 3–6 represent the start of the second-order regression that gave way to the final regression (Murayr Member). A first major sequence may be represented by the Sha'iba, Qasr and the lower part of the Subbat Members. It may be a double third-order sequence which corresponds probably in subsurface to Sequence S1 of Rahmani et al. (2002). The rest of the Jauf Formation may represent four third-order sequences and probably corresponds to the Sequence S2 of Rahmani et al. (2002).

2.3. Palaeontology in outcrop

The Sha'iba Member yielded brachiopods known from the Pragian and possibly also the Emsian (Boucot et al., 1989). Abundant fish debris were also found and appear to confirm the early Pragian age of these beds (Janjou et al., 1997a). The Qasr Member contains abundant fish remains that range from late Lochkovian to early Pragian (Janjou et al., 1997a). Boucot et al. (1989) also recovered conodonts in this unit indicative of middle Pragian to middle Emsian age and trilobites suggesting a Pragian to Emsian age range. The Subbat Member does not contain invertebrate fossils but one coarse-grained layer yielded rare undated vertebrate remains (Janjou et al., 1997a). The Hammamiyat Member is rich in vertebrate and invertebrate fossils, and contains several highly fossiliferous strata that yielded Emsian brachiopods (Bahafzallah et al., 1981; Boucot et al., 1989) and accompanying bryozoans, gastropods, bivalves, cephalopods, crinoids, and fish debris of minor stratigraphic interest. Some fish spines from the Hammamiyat Member are known only from the Emsian to Givetian from Gondwana (Lelièvre et al., 1995). The Murayr Member has several layers rich in vertebrate remains, two taxa of which are known in the Middle to Late Devonian. Fragments of *Prototaxites*, which is a tree-like fungus restricted to the Devonian, were collected in place throughout the Murayr Member. Remains of plants were also found in the argillaceous beds at the base of the member (Wallace et al., 1997).

Faunas and floras were thus collected from many fossiliferous beds throughout the Jauf Formation. Boucot et al. (1989) who studied samples from the Qasr and Hammamiyat members assigned a Pragian to early Emsian age to the Jauf Formation on the basis of brachiopods, trilobites, conodonts and fish remains. Forey et al. (1992) drew the same conclusion from fish remains found in the Jauf Formation. Janjou et al. (1997a) concluded that the collected faunas indicate an age ranging from Pragian (in the Sha'iba Member) to early or late Emsian (in the Hammamiyat Member); the Qasr Member being assigned to the Pragian. They stated that none of the vertebrate taxa found in the Jauf Formation is typically characteristic of the Eifelian. The palynological assemblages were also studied by various authors and their results are discussed in the following section.

3. Review of palynological studies

Loboziak and Streel (1995) were the first to publish palynological results from the Jauf Formation in northern Saudi Arabia. Based on taxa common to Euramerica, they applied the Devonian spore zonation developed for Western Europe by Streel et al. (1987) for the TRBH-1 borehole. They assigned the spore assemblages from the uppermost Tawil and lower Jauf formations to the Emsian, while the lower part of the Tawil Formation was dated as Late Silurian to Early Lochkovian (Steemans, 1995). Higher in the sequence, in the Subbat Member, Loboziak and Streel (1995) recognized a late Emsian spore assemblage.

Al-Hajri et al. (1999) published an operational palynological zonation developed by Saudi Aramco for Devonian strata for Saudi Arabia. Their work includes observations from the Jauf Formation in northern Saudi Arabia. They assigned a late Pragian–Eifelian age for the Jauf Formation. The biozonation was age-calibrated based on comparisons with the established spore zonations of Richardson and McGregor (1986) and Streel et al. (1987). Al-Hajri et al. (1999) identified the early Pragian–late Emsian D4A Palynosubzone from the lower part of the Jauf Formation and upper part of the underlying Tawil Formation in northwestern Saudi Arabia. The Emsian D3/D4 Palynozone is associated with the middle part of the Jauf Formation. These authors attributed the D3B Palynosubzone, which is widespread in Arabia, to the Hammamiyat and possibly the Subbat Members, and suggested a likely late Emsian age. The late Emsian-early Eifelian D3A Palynosubzone is defined in the upper Jauf and lower Jubah Formations.

In Breuer et al. (2005), the age of the Jauf Formation is assessed using index species from the established Euramerican Devonian palynozonations (e.g. Streel et al., 1987; Steemans, 1989). This showed that the Jauf Formation in northwestern Saudi Arabia ranges from late Pragian to latest Emsian. By correlating with the spore zonations of Richardson and McGregor (1986) and Streel et al. (1987), Al-Ghazi (2007) assigned an Emsian age to the partly cored Jauf Formation from an exploration borehole in northern Saudi Arabia. Recently, many new endemic species were described (Breuer et al., 2007; Breuer and Steemans, 2013). These authors determined a late Pragian to late Emsian age for the entire Jauf Formation in northern Saudi Arabia. In Breuer and Steemans (2013) the Jauf Formation extends from the *Synorisporites papillensis–Cymbohilates baqaensis* to the *Emphanisporites annulatus–Grandispora protea* Assemblage Zone. They subdivided the formation into four assemblages, three interval and one acme zones. These are described below in the biostratigraphy section.

4. Description of the palynological assemblages

Abundant and well-preserved palynomorphs were recovered from throughout the investigated Jauf sections. Most assemblages contain a mixture of terrestrial (spores, phytodebris and freshwater algae) and marine elements (acritarchs, prasinophytes, scolecodonts and very rarely chitinozoans). Some assemblages are dominated by spores and phytodebris, with marine elements generally rare or totally absent. Others are dominated by sphaeromorphs and/or acritarchs. In rare instances freshwater coenobial algae are predominant. The palynological assemblages are interpreted to reflect estuary, lagoonal to nearshore, shallow marine depositional conditions, characterized, in most cases, by a very high terrestrial sediment input, and variable marine influence. The characteristics and significance of these assemblages are discussed in detail below. All the spore taxa encountered in the sections are listed in the appendix, described and illustrated in Breuer et al. (2007), Breuer and Steemans (2013) or herein. Stratigraphic ranges of spore taxa, diversity curves for spores, cryptospores and marine palynomorphs, and relative abundance of each palynological group are plotted on Figs. 5 to 8.

4.1. Sha'iba Member

In the lower part of the Sha'iba Member in BAQA-2 (134.4 and 133.0 ft samples), the assemblages recovered from a marine bay depositional setting (Fig. 2) are rich, diverse, and composed of large numbers of miospores and acritarchs. The base of the Sha'iba Member was deposited during a transgressive, shallow-marine, nearshore setting over low local relief (Boucot et al., 1989). This bay-type environment succeeded the sandy deltaic system of the Tawil Formation. In this environment, trilete spores are diverse (more

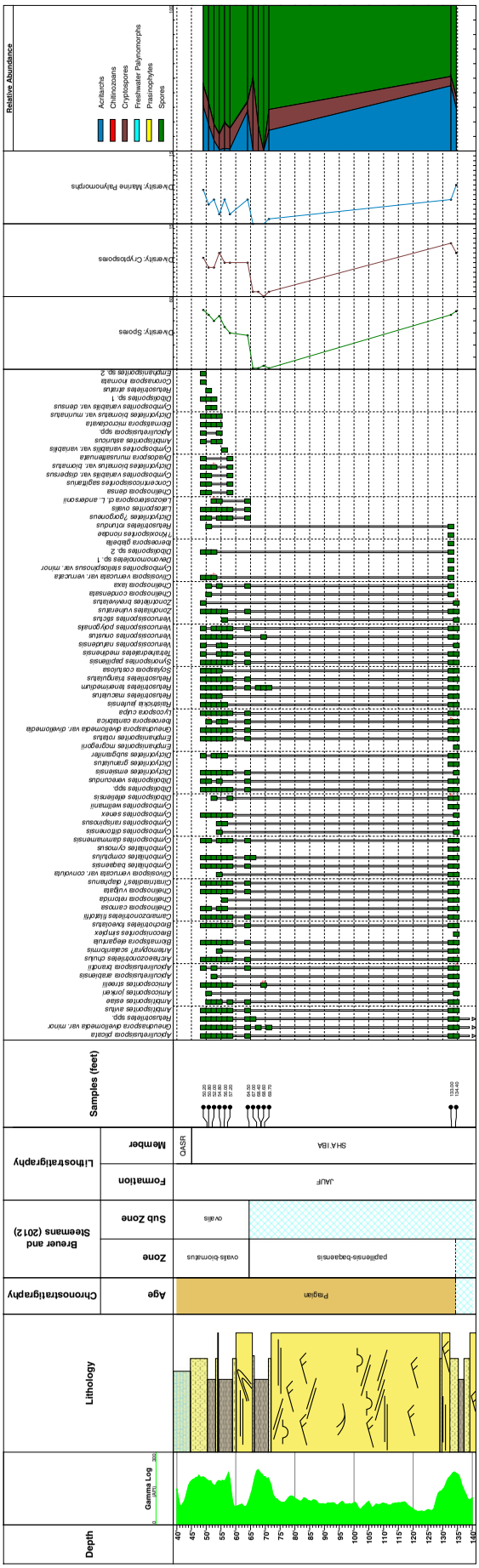

Fig. 5. Stratigraphic ranges of spore species, diversity and relative abundance of environmentally sensitive palynomorphs in BAQA-2.

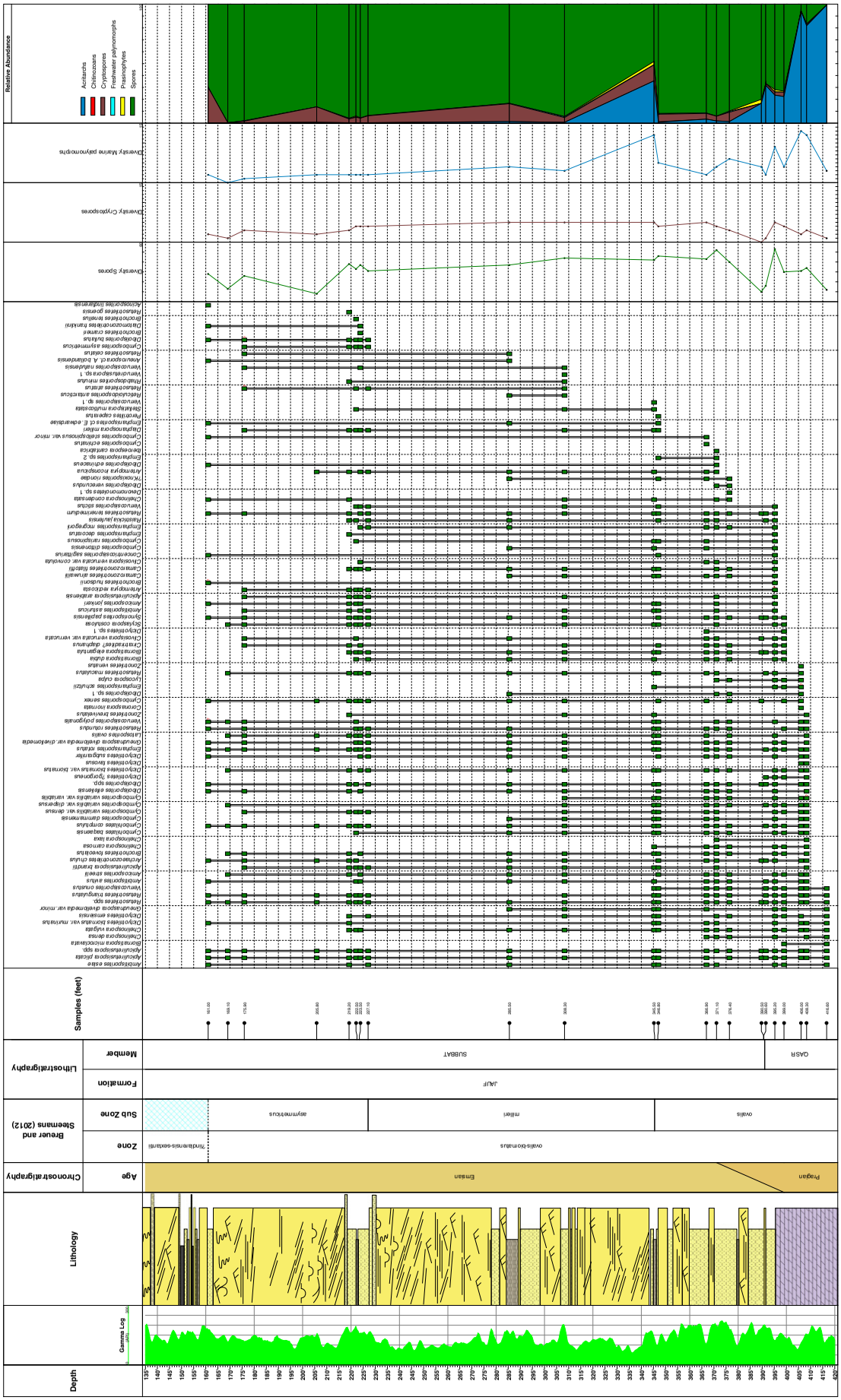

Fig. 6. Stratigraphic ranges of spore species, diversity and relative abundance of environmentally sensitive palynomorphs in BAQA-1.

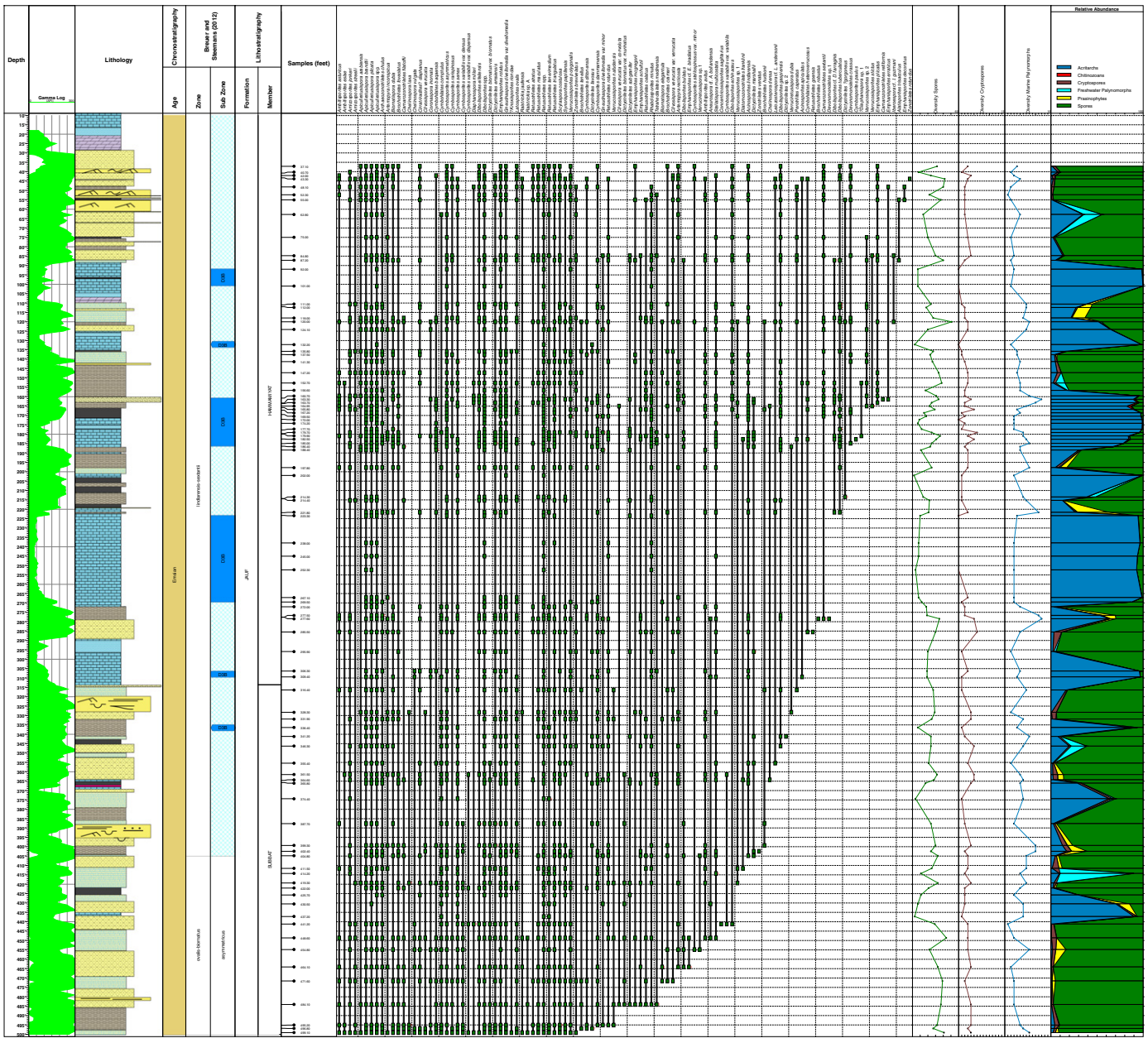

Fig. 7. Stratigraphic ranges of spore species, diversity and relative abundance of environmentally sensitive palynomorphs in JNDL-4.

than 45 different species) and dominant. They are represented by numerous specimens of *Apiculiretusispora plicata*, *Retusotriletes* spp. and *Synorisporites papillensis*. The other most characteristic trilete spores are *Ambitisporites avitus*, *Biornatispora elegantula*, *Camarozonotriletes filatoffii*, *Chelinospora carnosa*, *C. vulgata*, *Cirratriradites*? *diaphanus*, *Cymbosporites dammamensis*, *C. rarispinosus*, *C. wellmanii*, *Dictyotriletes subgranifer*, *Lycospora culpa*, *Raistrickia jaufensis*, *Scylaspora costulosa*, *Verrucosisporites onustus* and *V. polygonalis*. Cryptospores represent only 7–9% of the palynological assemblages but are diverse (9–11 species). They include above all hilate species such as *Cymbohilates baqaensis*, *C. comptulus* and *Gneudnaspora divellomedia* var. *minor*. Although miospores dominate the assemblages acritarchs may be locally numerous, represented mainly by *Gorgonisphaeridium* spp., *Multiplicisphaeridium* spp. and *Veryhachium* spp. These constitute more than 40% of the whole palynological assemblage in the 133.0 ft sample.

Higher, in the 69.7–67.0 ft interval, the samples yield low to moderate amounts of organic matter and are impoverished in palynomorphs (Fig. 5). The upper part of the Sha'iba Member (64.5–50.2 ft interval) yields an increase of organic matter and rich assemblages. In these sediments interpreted to have been deposited in lagoonal tidal flat (Fig. 2), the terrestrial component increases and varies from 69% to 98% of the palynological assemblage. Although *Apiculiretusispora plicata*, *Retusotriletes* spp., *Synorisporites papillensis* are still abundant, laevigate retusoid spores increase in numbers compared to the lower Sha'iba Member. In contrast with the lower Sha'iba Member the first occurrence of common species such as *Dictyotriletes* ?*gorgoneus*, *Latosporites ovalis*, *Leiozosterospora* cf. *L. andersonii* and members of the *Dictyotriletes biornatus* Morphon (see Breuer and Steemans, 2013), and the disappearance of *Cymbosporites wellmanii* and *Dictyotriletes granulatus* are the major differences. Cryptospores are slightly less diverse (6–9 species) than previously but increase up to 18% of the assemblage. *Gneudnaspora divellomedia* var. *minor* specimens are abundant. The other common cryptospores are *Cymbohilates baqaensis*, *C. comptulus* and *Zonohilates vulneratus*. Although the miospore

diversity increases up section in this interval (from 28 to 45), it is generally comparable to the lower part of the Sha'iba Member. Unlike the lower part of the Sha'iba Member, the marine component is mainly represented by leiospheres and some prasinophytes.

4.2. Qasr Member

In the Qasr Carbonate Member in BAQA-1, the palynological assemblages from the 416.6 to 406.0 ft interval reflect a shallow-marine/lagoon subtidal environment (Fig. 6). The proportionally lower number of miospores is interpreted to represent distance of source area. The palynological assemblages are dominated by acritarchs. In the stratigraphically deepest sample (416.6 ft), the marine assemblage is nearly monospecific and represented by abundant leiospheres. Stratigraphically above acritarchs become diverse with a dozen species belonging notably to *Diexallophasis* spp., *Gorgonisphaeridium* spp., *Multiplicisphaeridium* spp., *Polygonium* spp. and *Veryhachium* spp. and other acantomorphic genera. These acritarch species represent up to half of the marine palynomorph population in the 408.3 ft sample, the remainder being leiospheres.

4.3. Subbat Member

As progradation of the Subbat Member siliclastics over marine carbonates of the Qasr Member represent a regressive phase that succeeded the first transgressive episode at the base of the Jauf Formation, the spores become predominant from the 399.0 ft sample upwards in BAQA-1 (Fig. 6). The miospores reach their highest diversity (52–53 species) in the lower part of the Subbat Member. In this interval up to the 345.5 ft sample, the spores are mainly represented by species of the genera *Apiculiretusispora*, *Biornatispora*, *Chelinospora*, *Cymbosporites*, *Dictyotriletes*, *Emphanisporites*, *Retusotriletes*, *Synorisporites* and *Verrucosisporites*. The most common characteristic trilete spores are *Biornatispora elegantula*, *Camarozonotriletes alruwailii*, *Chelinospora carnosa*, *C. condensata*, *C. densa*, *Dictyotriletes biornatus* Morphon, ? *Knoxisporites riondae*, *Synorisporites papillensis*, *Verrucosisporites onustus* and *V. polygonalis*. Although most of these species are also known from the Sha'iba Member, they co-occur with rarer stratigraphically useful species that make their first appearance in this interval such as *Biornatispora dubia*, *Brochotriletes hudsonii*, *Diaphanospora milleri*, *Emphanisporites schultzii* and *Stellatispora multicostata*. Cryptospores are still dominated by *Cymbosporites baqaensis* and *C. comptulus*. The latter can be particularly abundant locally and reach up to 10% of the palynological assemblage. In the lower Subbat Member, the total amount of marine palynomorphs is low but increases up to 37% of the palynological assemblage at the top of this succession in the 345.5 ft sample with an influx of *Solisphaeridium* spp. specimens, which could represent a relative rise in sea level (Fig. 6). This could also be supported by the increase of acritarch diversity and the presence of rare chitinozoans (*Ramochitina magnifica* Lange 1967) in the 346.8 ft sample just below this acritarch-rich sample.

The middle to upper part of the Subbat Member in BAQA-1 (Fig. 2) corresponds to an estuary and was deposited in various subenvironments. The palynological assemblages from this interval (from 308.3 to 161.0 ft samples) show a very high terrestrial input as they include almost exclusively spores and cryptospores (Fig. 6). Trilete spores dominate the spore assemblages however cryptospores constitute a significant part throughout the upper part of the Subbat Member. Whereas the lower part of the Subbat Member is mainly characterized by spores with proximal papillae, emphanoid, verrucate, reticulate/foveolate and laevigate retusoid spores, these types of spores become less common towards the top of the section in BAQA-1. In the upper part of the Subbat Member, they are progressively replaced by numerous specimens of *Apiculiretusispora* and cryptospores. The stratigraphically useful species such as *Rhabdosporites minutus*, *Cymbosporites asymmetricus* and *Acinosporites lindlarensis* successively make their appearance in this sequence. Species that were common in the underlying sections have vanished such as *Chelinospora carnosa*, *Dictyotriletes* ? *gorgoneus*, *Lycospora culpa* and *Verrucosisporites onustus*.

In the Subbat Member the spore and cryptospore diversity decreases progressively to reach a minimum (8–30 species for spores and 1–3 species for cryptospores) in the 205.8–161.0 ft interval (Fig. 6). In these monotonous spore assemblages, relative abundance of cryptospores can reach up to 30% of the palynological assemblage. *Cymbosporites senex* and its cryptospore equivalent, *Cymbohilates comptulus*, which are probably produced by the same parent plant, are particularly abundant locally. Combined they constitute 24% to 48% of the palynological assemblage respectively in the 205.8 and 161.0 ft samples. The rest of spores mostly belong to species of the genera *Apiculiretusispora* and *Retusotriletes*. As these assemblages are not diverse, dominated by a few species and rich in cryptospores, it indicates that most of the dispersed miospores came from local vegetation and underwent short transport. These assemblages seem to correspond to the period of maximum regression in the Jauf Formation. Furthermore it is supported by the sedimentological study of these deposits corresponding to a bayhead delta depositional setting (Fig. 2).

The Subbat Member in the Al-Jawf area is more shale-dominated in contrast to the more sand-dominated lithofacies in the Baq'a area (Fig. 4). As the depositional environment of the Subbat Member in JNDL-4 was shallow-marine to nearshore, the difference is also reflected in the palynology assemblages. A mix of terrestrial, freshwater and marine palynomorphs are present in JNDL-4 while palynological assemblages from the equivalent section in BAQA-1 (see Fig. 4) are less diverse and comprise almost exclusively terrestrially derived palynomorphs (Fig. 6). In JNDL-4, the spores from the Subbat Member are mainly represented by specimens belonging to *Apiculiretusispora*, *Cymbosporites*, *Emphanisporites* and *Retusotriletes*. *Dictyotriletes biornatus* Morphon vanish in the Subbat Member. *Chelinospora* representatives also decrease and almost disappear before the base of the Hammamiyat Limestone Member. The main biostratigraphic indices that appear in this interval are the more geographically widespread *Acinosporites lindlarensis* and *Rhabdosporites minutus*. *Cymbosporites senex* and *Cymbohilates comptulus* are also quite common locally but not as abundant as in BAQA-1. Combined they can constitute generally up to 8% of the palynological assemblage, and rarely more frequent. Cryptospores are mainly represented by *Cymbohilates comptulus* and *Gneudnaspora divellomedia*. This latter species progressively increases in abundance throughout the Subbat Member and becomes dominant among cryptospores in the Hammamiyat Member. *Gneudnaspora divellomedia* specimens occur above all in the spore-rich assemblages, notably between the samples in the 389.0–341.0 ft interval. Although the spore diversity drops when marine palynomorphs increase in number, the general trend shows a slight decrease towards the top of the Subbat Member. The occurrence of several acritarch-rich events in the upper part of the Subbat Member reflect the resumption of a transgressive trend that led to deposition of the Hammamiyat Limestone Member. These marine assemblages are not very diverse and mainly characterized by *Dictyotidium* spp., *Gorgonisphaeridium* spp. and *Leiosphaeridia* spp. representatives. Near the top of the Subbat Member, the marine event in the 336.0 ft sample is dominated by *Leiosphaeridia 'jaufensis'* and corresponds to the D3B Palynosubzone of Al-Hajri et al. (1999). This biozone is actually an acme zone characterized by the sudden dominance of monospecific small leiospheres in the whole palynological assemblage. This leiosphere-rich assemblage or D3B palynofacies is very distinctive and constitutes the first of a series of several events in JNDL-4 (see below). Large prasinophytes are also common in the Subbat Member and can represent up to about 15% of the whole palynological assemblage. Coenobia can be super abundant locally (e.g. 414.2 ft sample) indicating a significant freshwater input.

4.4. Hammamiyat Member

The Hammamiyat Limestone Member represents the maximum flooding in the Jauf Formation and is characterized by offshore to tidal flat facies in addition to lagoon (Fig. 3). According to Al-Husseini and Matthews (2006), the facies succession records six transgression/regression cycles, with a generally regressive upward trend, corresponding to the six limestone units noted by Helal (1965) and Boucot et al. (1989). This pattern is also reflected by the palynological assemblages from JNDL-4 and JNDL-3. These display an alternation of leiosphere-rich and spore-rich intervals throughout the Hammamiyat Member (Figs. 7 and 8). The marine pulses can be correlated between the two cored sections on logs, sedimentology and palynology. The spore assemblages comprise simple sculptured spores (*Apiculiretusispora*, *Cymbosporites* and *Dibolisporites*), laevigate retusoid, and emphanoid spores. The other spore groups are rather rare or occur sporadically. Of importance is the first occurrence of *Camarozonotriletes sextantii* in the shale above the third limestone and can be locally abundant in the two last units. Common species such as *Amicosporites jonkeri*, *Camarozonotriletes filatoffii*, *Cymbosporites dammamensis*, *Dictyotriletes emsiensis*, *D. favosus* and *Stellatispora multicostata* disappear before the last limestone of the Hammamiyat Member. The spore diversity drops momentarily in leiosphere-rich levels but it is higher where leiospheres are accompanied by more diverse marine palynomorphs indicating a more open-marine depositional settings. Cryptospores are almost or totally absent in the marine palynomorph dominated intervals. They usually are more abundant in spore-rich intervals of the tidal flats where they can reach up to 10% of the assemblage. Whereas *Cymbohilates* seems to be preferentially more characteristic of the siliclastics from the Subbat Member, *Artemopyra* and *Gneudnaspora* are more numerous in the Hammamiyat Member with common *A. inconspiuca*, *A. recticosta* and *G. divellomedia* representatives. Marine assemblages are recurrent and occur as a series of pulses throughout the interval and highlight the transgressives phases of each cycle. There are a series of six main marine events whose assemblages are dominated by *Leiosphaeridia 'jaufensis'* and correspond to the D3B Palynosubzone of Al-Hajri et al. (1999) recognized in eastern Saudi Arabia. They are related to the six limestone units of the Hammamiyat Member and occur in the carbonate and/or in the overlying shale. In addition there is another leiosphere-rich event in the 202.0 ft sample in JNDL-4 but it is distinguished from the D3B palynofacies as the assemblage is dominated by a thin-walled leiosphere species and might have a different significance. The assemblages are usually poor in diversity in the D3B palynofacies. These peculiar, low-diversity assemblages probably indicate lagoonal environments. Nevertheless the diversity increases with the occurrence of *Gorgonisphaeridium*, *Multiplicisphaeridium*, *Polyedryxium*, *Veryhachium* specimens and prasinophytes in some levels indicating more open-marine conditions locally. In these levels, the diversity can reach up to about a dozen different marine palynomorph species and is the highest within the second and third units of the Hammamiyat Member. The increase in marine diversity is characterized in the overlying shale of the third limestone by the abundance of chitinozoans (undescribed *Angochitina* spp.), which are elsewhere absent except for some different chitinozoan species in the lower Subbat Member (see above). An influx of prasinophytes tends to occur where a higher marine diversity is present. Coenobia and *Quadrisporites* occurrences can be significant for indicating freshwater input during regressive phases of each cycle. These algae are dominated by coenobia and can locally constitute up to about 20% of the palynological assemblage (Fig. 7).

4.5. Murayr Member

The deposits of the Murayr Member belong to a regressive siliciclastic estuarine complex that succeeded the Hammamiyat Limestone Member (Fig. 3). It was deposited in a brackish and estuarine environment channels (Boucot et al., 1989). The lower part of the Murayr Member in JNDL-3 was deposited in a tidal flat environment (Fig. 3). The palynological assemblages from this interval (from 294.0 to 268.1 ft samples) show a high terrestrial influence and contrast from the underlying last D3B event from the Hammamiyat Member. They include almost exclusively spores and cryptospores (Fig. 8). The spore assemblages are mainly composed, in order of abundance, by representatives of *Apiculretusispora*, *Dibolisporites* and *Retusotriletes*. The most common species are *Apiculiretusispora plicata*, *Dibolisporites echinaceus* and *D. gaspiensis*. *Cymbosporites*, which is common in the underlying levels, have dramatically decreased. Reticulate/foveolate forms are totally absent. The spore diversity is rather low and varies from 13 to 23 species at most. Cryptospores are dominated by *Artemopyra* and *Gneudnaspora* and represent 2%–4% of the whole palynological assemblage. Marine palynomorphs are poorly diverse and constitute less than 5% of the assemblages. They are mainly represented by *Leiosphaeridia 'jaufensis'* and scolecodonts.

In the upper Murayr Member, palynological assemblages (from 258.7 to 220.60 ft samples) contain a mix of terrestrial, freshwater and marine palynomorphs (Fig. 8). These assemblages with a couple of thin carbonate beds highlight transgressive fluctuations that replaced estuarine sedimentation by brackish conditions. The spores dominate only in the 250.0 ft sample. Over the interval, they are still represented by *Apiculiretusispora*, *Dibolisporites* and *Retusotriletes* specimens. The widespread species *Emphanisporites annulatus* first occur near the top of the Jauf Formation while lots of species have disappeared. The spore assemblages are poorly diverse and the diversity has decreased again from the Hammamiyat Member. It is not higher than 17 species at most. Cryptospores are almost absent and only represented by rare *Gneudnaspora divellomedia* var. *divellomedia* specimens. The marine input increases in general as well as its diversity, which is comprised between four and eight different forms. The acritarch assemblages still include locally abundant *Leiosphaeridia 'jaufensis'* but not super abundant as in the Hammamiyat D3B intervals. The leiospheres are mainly accompanied by other acritarch types belonging to *Gorgonisphaeridium*, *Leiosphaeridia*, *Rugaletes* and *Saharidia*. Although freshwater algae are mainly represented by coenobia, the occurrence of thick-walled, operculate *Quadrisporites* is typical of the Murayr Member. The significant increase of the freshwater component in the palynological assemblages from the upper part of the Murayr Member seems to presage deposition of fluvial sandstones from the overlying Jubah Formation.

5. Biostratigraphy

Most studied assemblages have an abundant and diverse spore component. Spores are the most useful biostratigraphic tool for dating and correlation of the Saudi Arabian Early Devonian deposits, although the rare occurrences of chitinozoans are also useful. Acritarchs, however locally abundant, were not studied in detail and will be the subject of a future paper.

The stratigraphic palynology of the Jauf Formation presented in Breuer et al. (2005, 2007) was principally based on species that are common to the standard Euramerican zonations of Richardson and McGregor (1986) and Streel et al. (1987). All the Euramerican biozones were not recognized for the studied interval. Precise trans- and intercontinental correlations based on spores are sometimes challenging (Traverse, 2007). Due to intrinsic provincialism of plants, the two standard Devonian spore zonations defined by Richardson and McGregor (1986) and Streel et al. (1987) in Euramerica are sometimes difficult to apply to localities outside Euramerica (Breuer and Steemans, 2013). In addition, Rubinstein et al. (2005), Steemans et al. (2008) and Troth et al. (2011) among others showed that key spore taxa that are used zonally in both Euramerica and Gondwana do not all have coincident inceptions in both areas. Some are earlier (*E. annulatus* in Euramerica, *D. emsiensis* in Gondwana), others later (i.e. *Ancyrospora* and *Hystricosporites* in Gondwana) whereas others are approximately

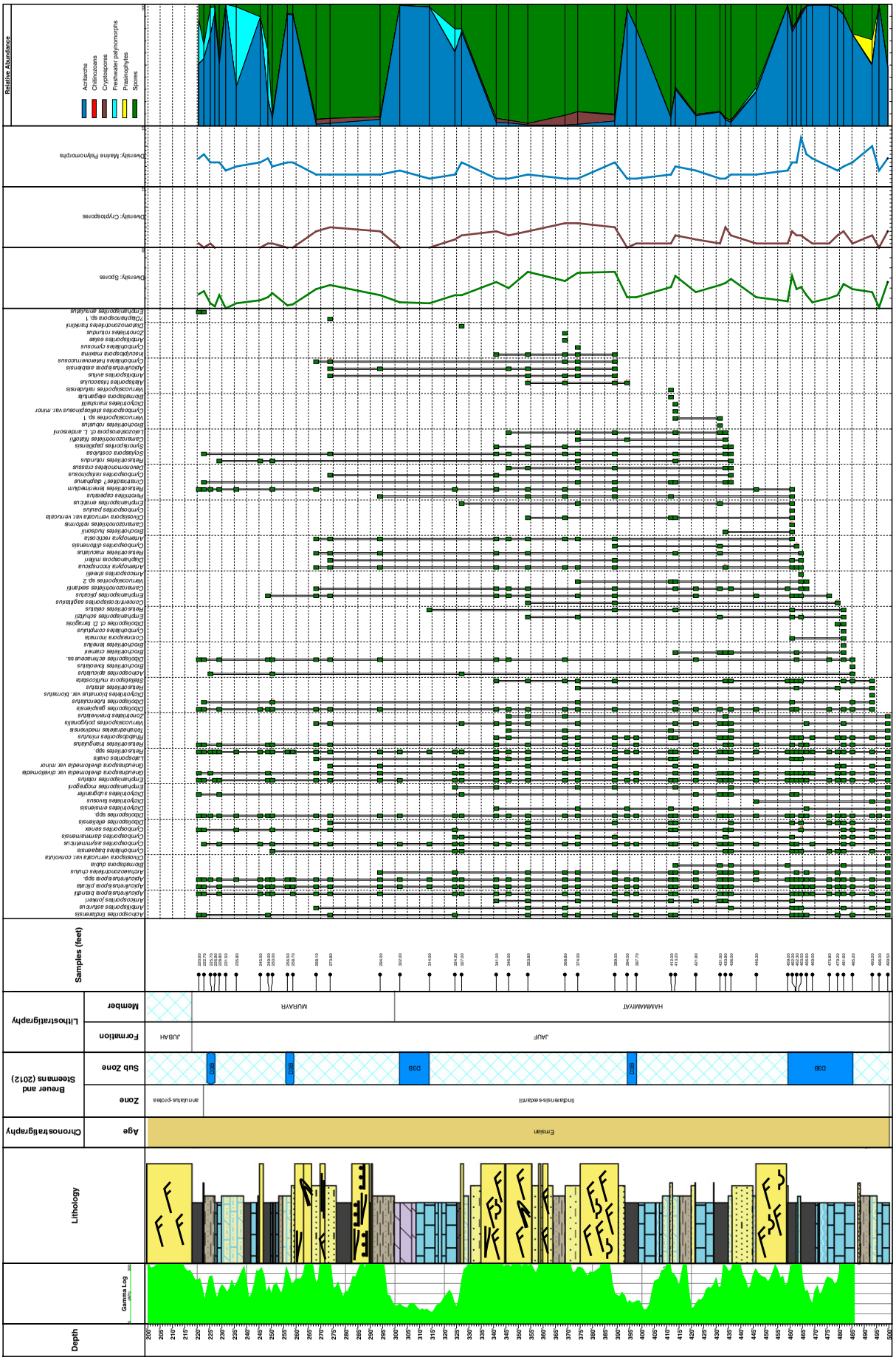

Fig. 8. Stratigraphic ranges of spore species, diversity and relative abundance of environmentally sensitive palynomorphs in JNDL-3.

synchronous (large *Grandispora* spp.). The biozonation of Breuer and Steemans (2013) defined in northern Gondwana allows a finer correlation for Saudi Arabian localities and better correlation with western Gondwanan and Euramerican localities. The palynostratigraphy of the Jauf Formation in the studied core holes is elucidated herein although the same sections were used by Breuer and Steemans (2013) to establish their biozonation.

The oldest spore assemblages from the lower part of the Sha'iba Member belong to *Synorisporites papillensis–Cymbohilates baqaensis* Assemblage Zone of Breuer and Steemans (2013) (Figs. 4 and 5). This zone is characterized by common *S. papillensis* specimens and well-diversified cryptospores including above all *C. baqaensis*, *C. comptulus* and *Gneudnaspora divellomedia* var. *minor*. The co-occurrence of *Verrucosisporites polygonalis* and *Dictyotriletes emsiensis* correlate this assemblage to the *polygonalis–emsiensis* Assemblage Zone of Richardson and McGregor (1986). The presence of *Dictyotriletes subgranifer* indicates more precisely the Su Interval Zone of Streel et al. (1987). Although the latter is spanning the Pragian/Emsian boundary, occurrence of species such as *Chelinospora retorrida* and *Dictyotriletes granulatus*, which are not recorded in the lower Emsian (Breuer and Steemans, 2013), indicate a late Pragian age for this section (Fig. 5).

In the upper Sha'iba, the first significant inception of monolete spores marks the base of the *Latosporites ovalis* Interval Zone from the *Latosporites ovalis–Dictyotriletes biornatus* Assemblage Zone of Breuer and Steemans (2013), which extends into the Subbat Member (Fig. 4). The simple monolete spore, *Latosporites ovalis*, is not very common, but a persistent component of the spore assemblages up to the top of the Jauf Formation (Breuer and Steemans, 2013). This occurrence is particularly interesting as it represents one of the earliest reports of a monolete spore, and hints at the possibility that monolete spores appeared on Gondwana, before their first appearance in Euramerica (Breuer et al., 2007). Monolete spores were also observed in coeval sediments from the Paraná Basin, Brazil (Mendlowicz Mauller, et al., 2007). *Dibolisporites echinaceus* sensu stricto and *Emphanisporites schultzii*, whose first appearance is known to be Emsian, combined with the last occurrences of *Chelinospora retorrida* and *Iberoespora cantabrica*, which are usually not younger than late Pragian, suggest that the Pragian/Emsian boundary lies within the *ovalis* Zone. The boundary is possibly picked in the uppermost Qasr or lowermost Subbat Member (Figs. 4 and 6). The presence of chitinozoans, *Ramochitina magnifica* Lange 1967, in the 346.8 ft sample (Fig. 4) indicates the *R. magnifica* Zone of Grahn (2005) defined in Western Gondwana. It is found in Antarctica, Argentina, Bolivia, Brazil, Paraguay and the Falkland Islands (see Troth et al., 2011). Although it is originally considered as Pragian (Gerrienne et al., 2001; Grahn, 2005), it is found within the Su Interval Zone in the Paraná Basin, Brazil (Grahn et al., 2010) and is thus in agreement with a late Pragian–early Emsian age for this part of the section.

The *Diaphanospora milleri* Interval Zone of Breuer and Steemans (2013) is recognized in the lower Subbat Member from BAQA-1 based on the first occurrence of the eponymous species (Figs. 4 and 6). Then the first inception of *Cymbosporites asymmetricus* indicates the *C. asymmetricus* Interval Zone of Breuer and Steemans (2013) in the middle part of the Subbat Member in BAQA-1 and JNDL-4 (Figs. 4, 6 and 7). The occurrence of *Rhabdosporites minutus* allows the partial correlation of the *Cymbosporites asymmetricus* Interval Zone to the Min Interval Zone of Streel et al. (1987) that is included in the FD Oppel Zone.

In upper Subbat Member from BAQA-1 and JNDL-4 (Figs. 4, 6 and 7), the first specimens of *Acinosporites lindlarensis* indicate the base of the middle-late Emsian *Acinosporites lindlarensis–Camarozonotriletes sextantii* Assemblage Zone of Breuer and Steemans (2013), which extends into the Murayr Member. *Camarozonotriletes sextantii* occurs afterwards above the third limestone from the Hammamiyat Member (Figs. 7 and 8). On the contrary, *C. sextantii*, which is a nominal species for the *annulatus–sextantii* Assemblage Zone of Richardson and McGregor (1986) and occurs in the AB Oppel Zone of Streel et al. (1987), appears before *A. lindlarensis* in Euramerica and as early as the early Emsian. The *lindlarensis–sextantii* Zone includes the D3B Palynosubzone of Al-Hajri et al. (1999), which represents a monospecific algal bloom. Although it is good marker horizon throughout Saudi Arabia (Al-Hajri et al., 1999), it is above all a distinctive palynofacies characterized by leiosphere-rich, low-diversity assemblages. D3B occurs in northwestern Saudi Arabia not as a unique event but a series of marine pulses that extends up to 400 ft thick (Breuer et al., 2007). The D3B marine assemblages alternate with terrestrial, spore-dominated assemblages.

The *Emphanisporites annulatus–Grandispora protea* Assemblage Zone of Breuer and Steemans (2013) is recognized in JNDL-3 based on the first appearance of *E. annulatus* from the 222.7 ft sample near the top of the Jauf Formation (Figs. 4 and 8). This assemblage zone is usually characterized by first occurrence of the large apiculate and spinose zonate–pseudosaccate spores (*Grandispora/Samarisporites* complex). Although absent in JNDL-3, first specimens of *G. protea* occur with *E. annulatus* in a coeval section from JNDL-1 (Breuer and Steemans, 2013). In JNDL-1, *E. annulatus* occurs slightly before *G. protea*. Interestingly, *E. annulatus* and *Grandispora* spp. (except the small *Grandispora* sp. A *in* Steemans et al., 2008, which occurs in the Lochkovian) have a near common inception in Bolivia (Troth et al., 2011), Ontario (McGregor and Camfield, 1976), North Africa and Saudi Arabia (Breuer and Steemans, 2013). The appearance of *E. annulatus* is well constrained to the lowermost Emsian, in northwestern Europe (Steemans, 1989; Streel et al., 2000) and Canada (Richardson and McGregor, 1986) whereas it is delayed to the upper Emsian in all Gondwana (e.g. Grignani et al., 1991; Melo and Loboziak, 2003; Troth et al., 2011; Breuer and Steemans, 2013) and even Ontario (Troth et al., 2011, p. 15). Besides, the first appearance of the large zonate–pseudosaccate spores (i.e. *Grandispora* spp.) is known globally in the upper Emsian and corresponds in Euramerica to the *douglastownensis–eurypterota* Assemblage Zone of Richardson and McGregor (1986) and the AP Oppel Zone of Streel et al. (1987), and in Western Gondwana to *Grandispora/Samarisporites* spp. Interval Zone of Melo and Loboziak (2003). In the German GSSP section (Riegel, 1982; Ziegler, 2000), where spores occur with both goniatites and conodonts, the first appearance of *Grandispora* spp. is latest Emsian in age. Consequently the top of the Jauf Formation is not younger than the latest Emsian.

6. Depositional model based on palynological assemblages

6.1. Data

In the Early Devonian section represented by the BAQA-1 and BAQA-2 core holes the secondary dolomitic portion of the Qasr Member contains numerous acritarch specimens and the number of miospore species is drastically reduced compared to the assemblages from the Sha'iba Member. The environment of deposition for this dolomitic interval is interpreted to be lagoonal. Among the miospore species that disappear during Qasr time, many reappear progressively in the overlying siliciclastic sediments, within the upper part of the Qasr and the Subbat members. Through this succession, the environment of deposition changes from lagoonal to estuarine. Fifteen of the 30 miospore species reappear progressively above the dolomitic Qasr: *Ambitisporites asturicus*, *Amicosporites jonkeri*, *Apiculiretusispora arabiensis*, *Camarozonotriletes filatoffii*, *Clivosispora verrucata* var. *convoluta*, *Cymbosporites dittonensis*, *C. rarispinosus*, *Raistrickia jaufensis*, *Retusotriletes tenerimedium*, *Chelinospora condensata*, *Devonomonoletes* sp. 1, *Dibolisporites verecundus*, *?Knoxisporites riondae*, *Emphanisporites* sp. 2 and *Iberoespora cantabrica*.

In JNDL-4, the palynological assemblages alternate between intervals dominated by miospores and those dominated by leiospheres (see above). Among the miospore species listed above several have a long stratigraphic range and are still present in the upper Subbat

and the Hammamiyat members. They are *Ambitisporites asturicus*, *Amicosporites jonkeri*, *Apiculiretusispora arabiensis*, *Camarozonotriletes filatoffii*, *Clivosispora verrucata*, *Cymbosporites dittonensis*, *C. rarispinosus*, *Raistrickia jaufensis*, *Retusotriletes tenerimedium* (i.e. nine of the 15 species listed above, reappearing in the lower Subbat Member). With rare exceptions, these nine species disappear from the leiosphere-dominated intervals and then reappear. There is one important anomalous leiosphere-rich event, which contains palynological assemblages different from the others (Fig. 7). Over the 160.7–188.4 ft interval, samples are rich in leiospheres but also contain miospores from the hinterland. An increase of marine palynomorph diversity and the presence of rare to common chitinozoans characterize this stratum (see above). This pattern biofacies succession is also observed in the coeval section from JNDL-3 (Fig. 8).

6.2. A possible interpretation

Classically, the Qasr Carbonate Member is interpreted to represent a maximum flooding (Sharland et al., 2001). The dolomitic portion of the Qasr in BAQA-1 indicates that detrital siliciclastic input is diminished. The numerous miospore species present are interpreted to have been derived from local vegetation. Species, which were thought to have been transported by rivers from the hinterland and observed below in the Sha'iba Member, disappear during this period in conjunction with a decrease in fluvial siliciclastics. They reappear above the dolomite where siliciclastic sediments are again transported into the basin. According to this hypothesis, the dolomitic horizon would not correspond to a maximum flooding but to an arid period during which the input of siliciclastics transported by rivers is very low. This hypothesis seems to be confirmed by observations of the Hammamiyat Member depositional environments from the JNDL-3 and JNDL-4 core holes where sediments are more carbonate-rich. Each depositional event in which hinterland species are absent corresponds to intervals of carbonate sedimentation and the concomitant occurrence of abundant leiospheres. This type of palynofacies is interpreted to reflect arid periods during which miospores, normally derived from the hinterland, are restricted by the lack of fluvial transport into the basin.

Fig. 9 summarizes the changes in depositional environments encountered in the Jauf Formation and their evolution through time. Several phases can be observed.

Phase 1. Rivers transport huge amount of sediments from the coastline up to the hinterland. Sediments are detrital and contain continental palynomorphs from the area transected by fluvial systems. Lowland derived miospore species are observed in the sediments along with those produced in the hinterland. Even though there is a low subsidence, it is largely compensated by siliclastic sediments prograding into the central basin. Phase 1 corresponds to a sedimentological system under a humid climate (estuary).

Phase 2. The climate becomes progressively drier. River systems partially disappear limiting sediment transport to the coastal plain. The shape of the coast line changes and a lagoon develops, probably because of subsidence. The climate is interpreted to be hot and dry allowing sedimentation of carbonates. Shale interbedded within the carbonates yield miospores derived from the immediate area. Hinterland miospores are not present in the lagoon as rivers cannot transport sediments to the coast. Under a dry and warm climate, the depositional environment may be eutrophized and responsible for blooms of algae (e.g., Strother, 1994), corresponding to the D3B palynofacies.

Phase 3. The climate becomes more humid resulting in increased amounts of siliciclastic sediments transported by rivers from the coastal plain and the hinterland. Carbonate sediments decrease in quantity and extent. Siliciclastic sediments prograde and form an estuarine environment. They contain miospores from lowland plain and hinterland biotopes and locally significant amounts of freshwater algae. Phase 3 is similar to Phase 1.

Phases 1 and 2 are cyclic and repeated several times, with minor differences. A lagoon is not always developed during Phase 2.

Phase 4. The subsidence rate vs. sedimentation rate changes drastically, allowing a flooding of the low land by the sea. This could be due to a stronger dry period, decreasing the input of sediments to the basin. In the Hammamiyat Member, this phase is characterized by palynological assemblages retrieved from the third limestone unit and the overlying shaly interval, corresponding to the 160.7–188.4 ft interval (Fig. 7). Contrary to the earlier D3B events, palynological samples contain miospore species representative of hinterland biotopes. The presence of those species in the shale layers interbedded with the carbonates suggests an important transgressive period, which corresponds to the D20 MFS of Sharland et al. (2001). In this phase the shoreline is closer to the biotopes where the hinterland plants where growing reducing the transport distance to the sedimentary basin. Miospore species are represented from all the biotopes.

Combining the lithofacies and the palynofacies represented by different terrestrial biotopes and marine assemblages provide data that lead to an integrated depositional model. It incorporates palaeoclimatic signals that explain the causes of basinal evolution and can be used to infer the significance of palynofacies.

6.3. Orbital signature

The Jauf Formation is described as an orbital second-order depositional sequence limited at the base by the second-order Tawil/Jauf boundary and at the top by the second-order Jauf/Jubah boundary (Al-Husseini and Matthews, 2006). The Jauf Formation would represent ca. 14.6 Ma. It consists of six third-order sequences and the Hammamiyat Member consists of six fourth-order orbital cycles each representing 0.405 Ma (Al-Husseini and Matthews, 2006).

According to new palynological data, the base of the Jauf Formation is close to the Pragian/Emsian boundary (407.0 ± 2.8 Ma) and the top of the analysed sequence (inside of the Murayr Member) is close to the Emsian/Eifelian boundary (397.5 ± 2.8 Ma). This indicates that the studied interval spans ca. 10 Ma and that the estimated 14.6 Ma duration for the Jauf Formation by Al-Husseini and Matthews (2006) could have been overestimated. Around thirty climatic cycles are observed throughout the Jauf composite section. This value, however, is constrained by sampling density; therefore, it represents a minimum. There is some uncertainty about the absolute ages used to make reliable hypotheses about the causes of that cyclicity and its effects on palynofacies and sedimentation.

An approach to estimating absolute age is to divide the duration of stages present by the number of miospore biozones. In the Jauf and the Jubah formations eleven miospore biozones have been defined (Breuer, 2007), from the Pragian/Emsian boundary up to the Givetian upper boundary (385.3 ± 2.6 Ma), a range of time of about 22 Ma. Therefore, each biozone would span ca. 2 Ma. The Jauf Formation is subdivided into five biozones over approximately 10 Ma. The estimate of 2 Ma per biozone seems to be realistic from these estimates. According to Al-Husseini and Matthews (2006) the Hammamiyat Member is estimated to be ca. 2.4 Ma, but we also know that duration of the Jauf Formation could have been overestimated by ca. 40%. Therefore, the Hammamiyat Member should be ca. 1.5. As the Hammamiyat Member represents approximately two thirds of the *lindlarensis–sextantii* Zone of Breuer and Steemans (2013), the biozone should be about 2.2 Ma. Despite

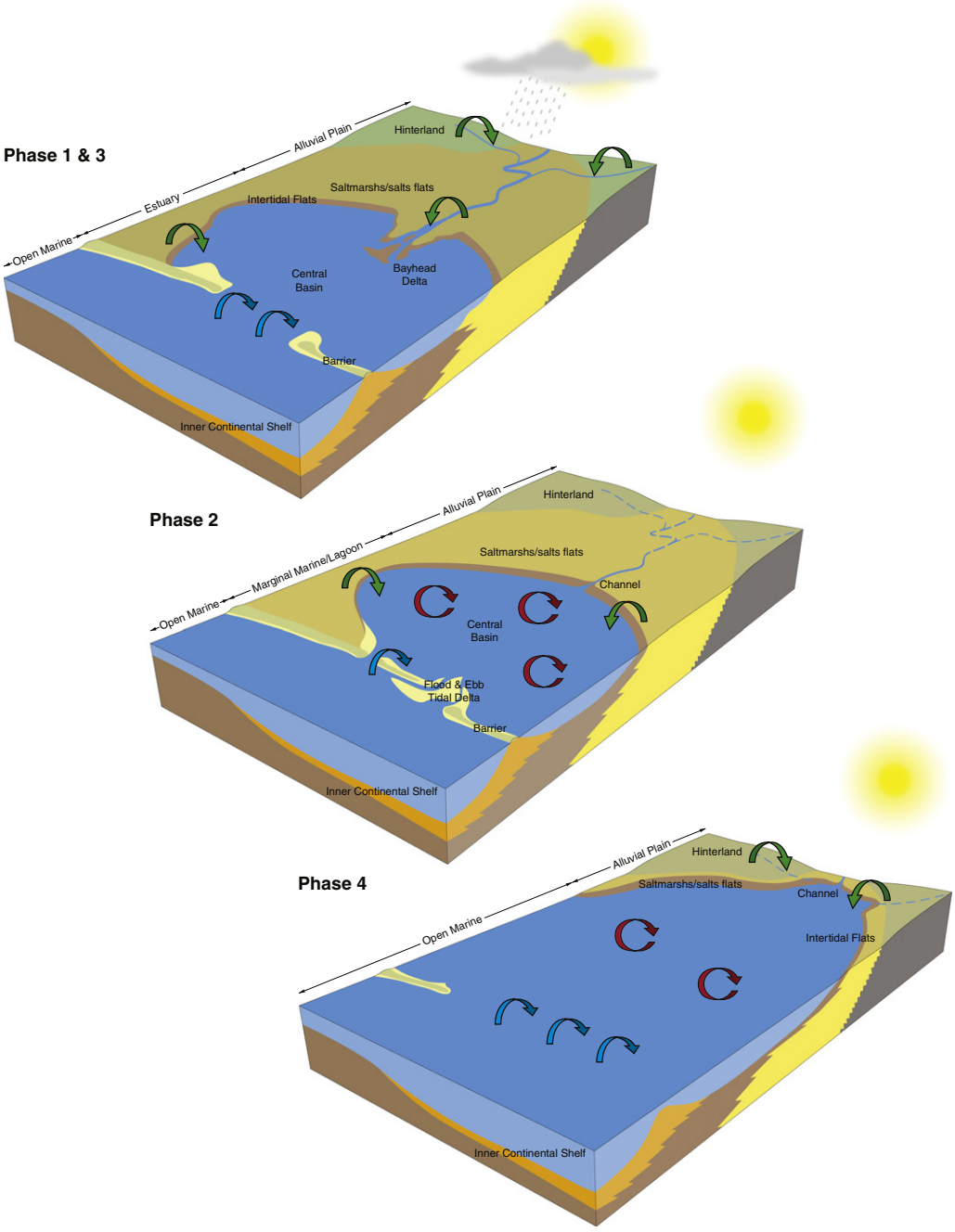

Fig. 9. Block diagrams summarising the distribution of the different environments in the Jauf Formation. Green arrow, spore input; blue arrow, marine acritarch input; red arrow, leiosphere bloom.

the limitations of these arguments, it would seem that the estimate of ca. 2–2.2 Ma for the *lindlarensis–sextantii* biozone is realistic.

According to the palaeogeographic and palaeoclimatic maps of Scotese (2000), during the Early Devonian time the Arabian Plate was on the northwestern border of the Gondwana at about 45°S. The boundary between an arid climate and a warm/wet climate latitudinally crosses at the position of Saudi Arabia. Around twenty climatic cycles may be recognized in the *lindlarensis–sextantii* biozone (i.e. around 100 ka for each cycle). This corresponds to the orbital eccentricity of Milankovitch cycles. The depositional model proposed here based on palynological observations could be a proxy for identification of orbitally-driven sedimentary cycles. We realize that this hypothesis is based on minimal data but feel that it has merit and should be tested as more data become available.

7. Conclusions

This paper synthesizes the results of palynological studies begun some time ago (Breuer et al., 2005, 2007; Breuer and Steemans, 2013) to refine the age of the Jauf Formation in northwestern Saudi Arabia. The new northern Gondwanan biozonation developed in Breuer and Steemans (2013) allows a fine regional correlation and larger-scale correlation with Gondwanan and Euramerican localities. Troth et al. (2011) showed that key spore used zonally in both Laurussia and Gondwana do not all have coincident first appearances in both areas, it is more

appropriate to apply regional biozonations to assess the age of the sections studied here rather than trying to apply the standard biozonations established in Euramerica such as Richardson and McGregor (1986) or Streel et al. (1987). We now realize, based on studied Arabian Plate sections, that some species such as *Camarozonotriletes sextantii* and *Emphanisporites annulatus* occur later in Gondwana than in Euramerica whereas others such *Acinosporites lindlarensis*, *Dictyotriletes subgranifer* and large *Grandispora* spp. are approximately synchronous.

Detailed palynological biostratigraphy confirms that the Jauf Formation is late Pragian to latest Emsian in age (Fig. 4). Four spore assemblage zones including three interval zones of Breuer and Steemans (2013) are defined for the Jauf Formation. The base of the Jauf Formation is late Pragian according to the occurrences of *Chelinospora retorrida*, *Dictyotriletes granulatus* and *D. subgranifer*. The top of the Jauf Formation is not younger than the latest Emsian based on the first appearance of *Emphanisporites annulatus* and *Grandispora protea* just below the base of the Jubah Formation. While chitinozoans from the Hammamiyat Member seem endemic to Saudi Arabia and do not allow any correlation, those from the lowermost part of the Subbat Member indicate the late Pragian–early Emsian *Ramochitina magnifica* Zone of Grahn (2005) defined in Western Gondwana. The Pragian/Emsian boundary is most likely within the upper part of the Qasr or lowermost Subbat Member as recognized using spores.

In addition, the palynological assemblages reflect the Jauf Formation depositional sequences. The rich and diverse assemblages from the Sha'iba Member, which is characterized by estuary to tidal flat environments, comprise mainly spores and acritarchs. The spores are dominant and diverse in this unit. These are replaced by acritarch-rich assemblages of the Qasr Member that indicate a major transgression with shallow-marine/lagoon subtidal environments. The palynological assemblages highlight the D10 Maximum Flooding Surface (MFS) of Sharland et al. (2001). Succeeding the marine Qasr Member, palynological assemblages of the Subbat Member represent a regressive phase as the spores again become dominant. Poorly diverse assemblages but rich in cryptospores in the middle part of the Subbat Member correspond most likely to a period of maximum regression in the Jauf Formation. The occurrences of several acritarch-rich events in the upper part of the Subbat Member reveal the resumption of a transgressive trend in which a series of D3B events were deposited during Hammamiyat Member time. Although the D3B Palynosubzone of Al-Hajri et al. (1999), which represents a monospecific algal bloom, ranges from the uppermost Subbat almost to the top of Jauf Formation within the Murayr Member, it is above all characteristic of the Hammamiyat Member and mainly restricted to the limestone intervals. This specific palynofacies is characterized by leiospherid-rich, low-diversity assemblages and occurs in northwestern Saudi Arabia not as a unique event but a series of marine pulses that are present over 400 ft (122 m) (Breuer et al., 2007). These isochronous pulses can be correlated with the fourth order cycles of Al-Husseini and Matthews (2006) recognized from outcrop. The transgressive marine leiosphere-rich assemblages alternate with spore-dominated assemblages, which represent brief regressive phases of the cycles. The palynological assemblage from the black shale interval overlying the third Hammamiyat limestone represents the D20 MFS of Sharland et al. (2001). It contains a diverse marine assemblage and the only rich chitinozoan level in the Devonian in Saudi Arabia. Sharland et al. (2001) identify the D20 MFS at the top of the first limestone unit while Al-Husseini and Matthews (2006) consider the maximum flooding interval at the second limestone. Succeeding the Hammamiyat Member, the assemblages from the Murayr Member reflect the general regressive trend that ultimately led to the deposition of fluvial sandstones of the Jubah Formation although they show some minor transgressive fluctuations. Indeed palynological assemblages become poorly diverse and contain a mix of terrestrial, freshwater and marine palynomorphs. They are transitional between the marine assemblages of the Hammamiyat Member and the continental assemblages from the lower Jubah Formation.

Acknowledgments

The authors would like to express their gratitude to management of the Saudi Arabian Ministry of Petroleum and Mineral Resources and the Saudi Arabian Oil Company (Saudi Aramco) for granting permission to publish this paper. They also acknowledge M. Giraldo-Mezzatesta and Prof. F. Boulvain (Liège University, Belgium) respectively for the preparation of palynological slides and comments on the depositional model presented herein. Thanks are especially expressed to Dr. B. Owens and an anonymous referee for comprehensively reviewing the manuscript.

Appendix A. Material and methods

The studied core holes are located in northwestern Saudi Arabia (Fig. 1). They include BAQA-1, BAQA-2, JNDL-3 and JNDL-4 core holes that in combination give a complete section through the Jauf Formation (Fig. 4). The preliminary palynological results from these core holes were published by Breuer et al. (2005, 2007) and the detailed taxonomy by Breuer and Steemans (2013). Palynological slides from these previous studies were re-examined and complemented by new samples resulting in a total of 175 productive samples. Although the majority of spore species from the studied assemblages were previously described, some are new and described below. After the first observation and the identification of species, which compose the palynological assemblages, quantitative species counts were carried out for each sample. At least 250 spore specimens per slide were counted when recovery was sufficient. Independently freshwater algae, acritarchs and other marine palynomorphs (prasinophytes, scolecodonts and chitinozoans) were also counted to determine their relative percentages and diversity.

All samples were processed according to standard palynological laboratory methods (Streel, 1965). Each sample was crushed and 10–25 g were demineralized in 10% HCl and 40% HF. The residue of the most thermally mature samples was oxidized in 65% HNO_3 and $KClO_3$ (Schultze solution) and sieved through a 10 μm mesh. Subsequently, a hot bath in 25% HCl eliminated the remaining fine neoformed fluoride particles. The residue of all samples was sieved through a 10 μm mesh. The final residue was mounted on palynological slides using Euparal or Eukit® resin. One to three slides were prepared for each productive sample.

All material is housed in the collections of Palaeobiogeology, Palaeobotany and Palaeopalynology at the Liège University and the collections of the Centre for Palynology of the University of Sheffield.

Appendix B. Systematic palaeontology

New species of cryptospores, monolete and trilete spores that were not described in Breuer and Steemans (2013) are described below and illustrated in Plates I to IV. Taxonomic descriptions are arranged alphabetically by genus and species within each group. The remainder of the taxa encountered in the studied sections are described and illustrated in Breuer et al. (2007) and Breuer and Steemans (2013).

Cryptospores

Genus ***Artemopyra*** Burgess and Richardson, 1991 emend. Richardson, 1996

Type species: *Artemopyra brevicosta* Burgess and Richardson, 1991.

Artemopyra? scalariformis Richardson, 1996 (Plate I, 1–2)

1996 *Artemopyra? scalariformis* Richardson, 1996: p. 18; pl. 10, Figs. 10–12.

Dimensions: 41 (42) 43 μm; 2 specimens measured.

Occurrence: BAQA-2; Sha'iba Member; *papillensis–baqaensis* Zone.

Genus ***Zonohilates*** gen. nov.

Type species: *Zonohilates vulneratus* gen. et sp. nov.

Derivation of name: Refers to the equatorial structure of the spore; from the Latin *zona*, meaning thin outer structure of a spore that projects at the equator.

Diagnosis: Hilate cryptospore monads with a proximo-equatorial thin zona or flange. Distal exine laevigate.

Zonohilates vulneratus gen. et sp. nov. (Plate I, 3–8)

Holotype: BAQA-2 core hole, sample 64.5 ft, slide 66818, Q38 (Plate I, 5).

Paratype: BAQA-2 core hole, sample 54.8 ft, slide 66815, L24 (Plate I, 3).

Locus typicus and stratum typicum: BAQA-2 core hole, Sha'iba Member of the Jauf Formation at Baq'a, Saudi Arabia.

Derivation of name: Refers to the characteristic of the flange; from the Latin *vulneratus*, meaning damaged.

Diagnosis: A *Zonohilates* species with a thin, proximo-equatorial flange irregular in outline.

Description: Amb is circular to sub-circular. A diffuse to distinct curvatura delimits a circular hilum. The proximal surface is often torn and shows different types of tears such as simple slits or more rarely a trilete-like configuration. The hilum is approximately seven-tenths to four-fifths of the amb diameter. Exine of the central body is punctate, thinner proximally, 2–3 μm thick equatorially and distally. The proximo-equatorial flange, generally up to about 10 μm wide, is always damaged and irregular. Proximal and distal surfaces are laevigate.

Dimensions: 38 (54) 70 μm; 18 specimens measured.

Remarks: The proximo-equatorial flange is probably damaged when the dyads are separated into monads. Although *Cirratriradites*? *diaphanus* Steemans, 1989 is trilete and has proximal papillae developed on each interradial area, it is quite similar to *Zonohilates vulneratus* in other respects. Both forms could have been produced by the same parent plant.

Occurrence: BAQA-2; Sha'iba Member; *papillensis–baqaensis* to *ovalis* zones.

Monolete spores

Genus ***Devonomonoletes*** Arkhangelskaya, 1985

Type species: *Devonomonoletes microtuberculatus* (Chibrikova) Arkhangelskaya, 1985.

Devonomonoletes crassus sp. nov. (Plate I, 9–15)

Holotype: JNDL-4 core hole, sample 167.2 ft, slide 68629, M28/1 (Plate I, 13).

Paratype: JNDL-4 core hole, sample 165.8 ft, slide 68628, M27/3 (Plate I, 10).

Locus typicus and stratum typicum: JNDL-4 core hole, Hammamiyat Member of the Jauf Formation at Domat Al-Jandal, Saudi Arabia.

Derivation of name: Refers to the general appearance of the spore; from the Latin *crassus*, meaning thick.

Plate I. Each figured specimen is identified by core hole, sample depth, slide number and England Finder Co-ordinate location. All figured specimens are at magnification ×1000.

1–2. *Artemopyra*? *scalariformis* Richardson, 1996.
1. BAQA-2, 134.4 ft, 66826, H36.
2. BAQA-2, 133.0 ft, 66825, V24/3.
3–8. *Zonohilates vulneratus* gen. et sp. nov.
3. Paratype, BAQA-2, 54.8 ft, 66815, L24.
4. BAQA-2, 56.0 ft, 66816, X34/1.
5. Holotype, BAQA-2, 64.5 ft, 66818, Q38.
6. BAQA-2, 64.5 ft, 66818, E29.
7. BAQA-2, 64.5 ft, 66818, J46/3.
8. BAQA-2, 133.0 ft, 66825, U29.
9–15. *Devonomonoletes crassus* sp. nov.
9. JNDL-4, 120.0 ft, 68612, R42.
10. Paratype, JNDL-4, 165.8 ft, 68628, M27/3.
11. JNDL-4,141.3 ft, 68619, F46/2.
12. JNDL-4, 55.0 ft, 68596, Q32.
13. Holotype, JNDL-4, 167.2 ft, 68629, M28/1.
14. JNDL-3, 353.8 ft, 68559, J51.
15. JNDL-4, 84.8 ft, 68603, D43/4.

Plate II. Each figured specimen is identified by core hole, sample depth, slide number and England Finder Co-ordinate location. All figured specimens are at magnification ×1000 (see on page 206).

1–8. *Camarozonotriletes alruwailii* sp. nov.
1. Holotype, BAQA-1, 395.2 ft, 66807, K22/1.
2. BAQA-1, 345.5 ft, 66794, H42/4.
3. BAQA-1, 346.8 ft, 66797, W48/4.
4. BAQA-1, 395.2 ft, 66807, J33.
5. BAQA-1, 395.2 ft, 66807, Q26/4.
6. Paratype, BAQA-1, 395.2 ft, 66807, S23/4.
7. BAQA-1, 395.2 ft, 03CW121, J37/1.
8. BAQA-1, 395.2 ft, 66807, C51.
9–10. *Cymbosporites paulus* McGregor and Camfield, 1976.
9. JNDL-4, 182.5 ft, 68836, L42.
10. JNDL-3, 462.0 ft, 68576, N51/2.
11–12. ?*Diaphanospora* sp. 1.
11. JNDL-4, 152.7 ft, 68622, V46.
12. JNDL-3, 273.8 ft, 68548, M44.
13–18. *Dibolisporites* cf. *D. farraginis* McGregor and Camfield, 1982.
13. JNDL-4, 182.5 ft, 68636, P34/3.
14. JNDL-4, 179.9 ft, 68635, U40.
15. JNDL-4, 163.7 ft, 68626, L32/1.
16. JNDL-4, 152.7 ft, 68622, F48.
17. JNDL-4, 167.2 ft, 68629, C29.
18. JNDL-3, 479.2 ft, 68582, C46.

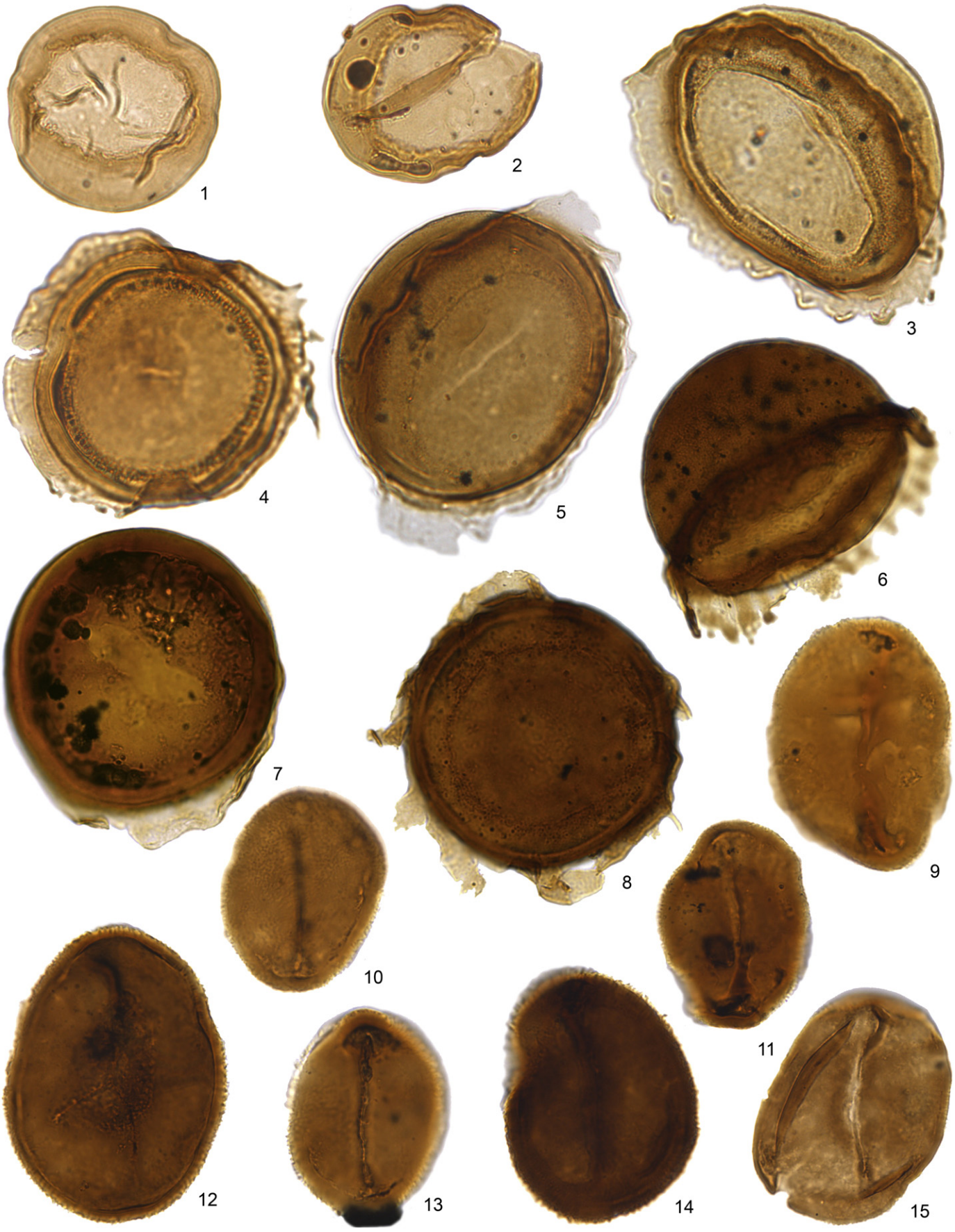
1
2
3
4
5
6
7
8
9
10
11
12
13
14
15

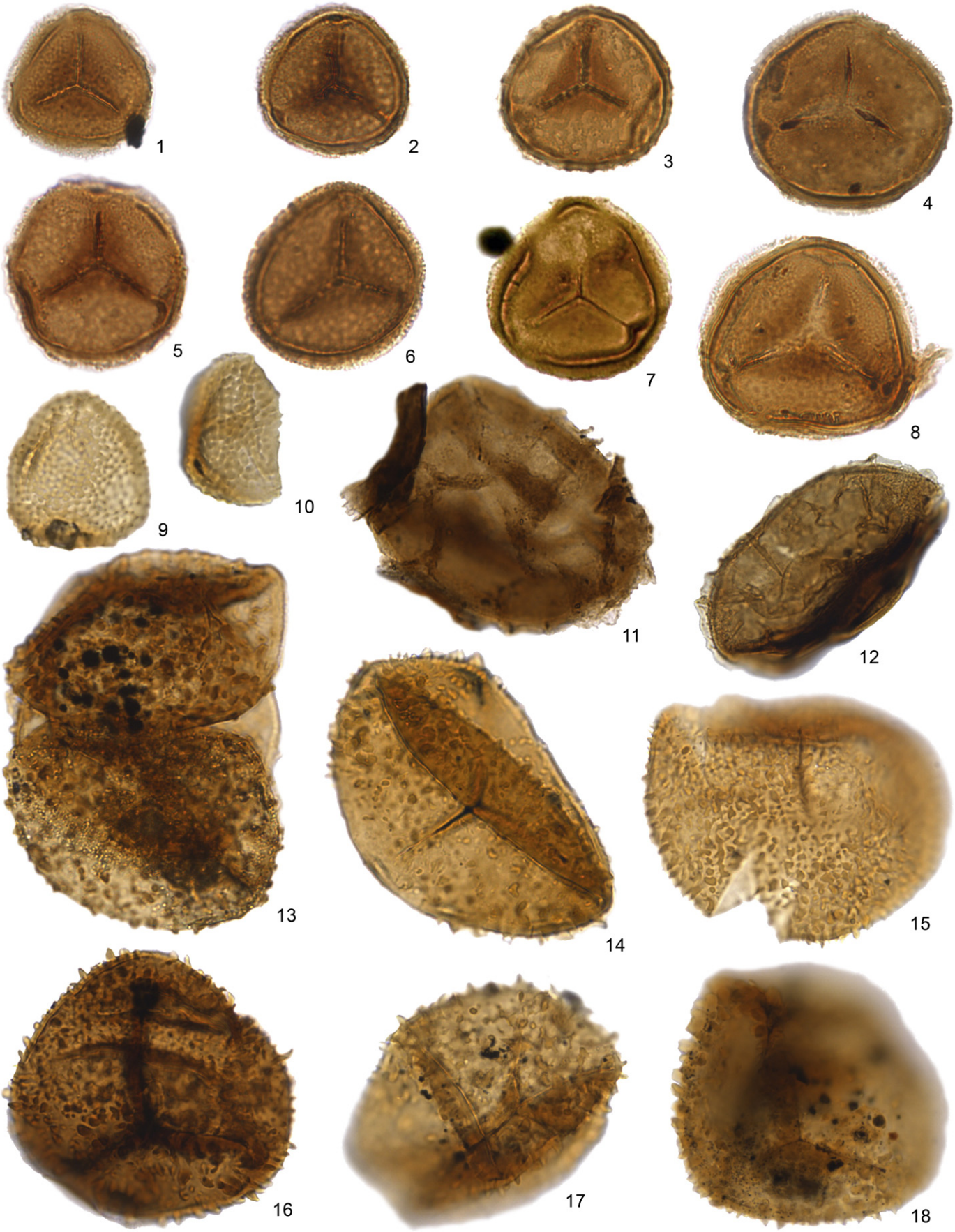

Plate II. (*caption on page 204*)

Diagnosis: A *Devonomonoletes* species with a sturdy appearance and sculptured with small, densely distributed coni and spinae.

Description: Amb is elliptical to oval. The length of the short axis generally equals seven-tenths to four-fifths of the long axis. Laesura is distinct, straight to slightly curved, accompanied by prominent labra commonly 1-3 μm in overall width, and terminating in well-defined curvaturae. Exine is 1.5–4.0 μm thick. Proximo-equatorial and distal regions are sculptured with evenly and densely distributed coni and spinae c. 1 μm high. Contact faces are laevigate.

Dimensions: 40 (45) 50 μm; 19 specimens measured.

Remarks: Although *Cymbosporites asymmetricus* Breuer et al., 2007 is trilete, it is also elongate and has a similar ornamentation. Some specimens of *Devonomonoletes crassus* (e.g. Plate I, 12) have what appears to be an additional laesura that resembles the asymmetrical trilete mark of *C. asymmetricus*.

Occurrence: JNDL-3 and JNDL-4; Hammamiyat Member; *lindlarensis–sextantii* Zone.

Trilete spores

Genus ***Camarozonotriletes*** Naumova, 1939 ex Naumova, 1953

Type species: *Camarozonotriletes devonicus* Naumova, 1953.

Camarozonotriletes alruwailii sp. nov. (Plate II, 1–8)

Holotype: BAQA-1 core hole, sample 395.2 ft, slide 66807, K22/1 (Plate III, 1).

Paratype: BAQA-1 core hole, sample 395.2 ft, slide 66807, S23/4 (Plate III, 6).

Locus typicus and stratum typicum: BAQA-1 core hole, Subbat Member of the Jauf Formation at Baq'a, Saudi Arabia.

Derivation of name: Named in honor of Mansour Al-Ruwaili, Saudi Aramco palynologist, who retired in 2011.

Diagnosis: A *Camarozonotriletes* species sculptured with minute, closely spaced grana, coni or spinae. Cingulum width opposite the laesurae slightly reduced.

Description: Amb is sub-circular to sub-triangular. Laesurae are simple, straight, commonly three-fifths to three-quarters of the amb radius in length. Exine along laesurae is dark and presumably represents a triangular thickened zone, wider near the proximal pole and tapering towards the equator. Curvaturae are visible and often correspond interradially to the inner margin of the cingulum. Cingulum is 1–2 μm thick equatorially opposite the laesurae and 1.5–3.0 μm thick interradially. Exine is laevigate proximally. Distal and equatorial sculpture are composed of closely spaced grana, coni or spinae, generally up to 1 μm high and 0.5 μm wide. The largest elements occur in the equatorial interradial region.

Dimensions: 27 (35) 45 μm; 16 specimens measured.

Remarks: Reduction of the cingulum width opposite the laesurae is not often conspicuous in some specimens. Sculptural elements are not always evenly distributed. Some laevigate spots and convolute zones can occur distally on some specimens (e.g. Pl. 2, 2–3, 6).

Comparison: *Camarozonotriletes parvus* Owens, 1971 is thicker equatorially and sculptured with smaller elements often barely perceptible. Specimens described as *C. parvus* in Steemans (1989), which are misidentified and represent actually a different species (Breuer and Steemans, 2013), are thicker interradially. Besides their sculpture comprise higher bacula, pila and spinae.

Occurrence: BAQA-1; Subbat Member; *ovalis* to *milleri* zones.

Genus ***Cymbosporites*** Allen, 1965

Type species: *Cymbosporites cyathus* Allen, 1965.

Cymbosporites paulus McGregor and Camfield, 1976 (Plate II, 9–10)

1976 *Cymbosporites paulus* McGregor and Camfield: p. 15; pl. 2, Figs. 7–9.

Dimensions: 30 (30.5) 31 μm; 2 specimens measured.

Occurrence: JNDL-3 and JNDL-4; Hammamiyat Member; *lindlarensis–sextantii* Zone.

Genus ***Diaphanospora*** Balme and Hassell, 1962

Type species: *Diaphanospora riciniata* Balme and Hassell, 1962.

?*Diaphanospora* sp. 1 (Plate II, 11–12)

Description: Amb is sub-circular. Laesurae are not perceptible. Nexine is granulate, c. 1 μm thick. Sexine extremely thin, transparent, closely appressed to the spore body and showing local detachment at the equator. Sexine surface folded in a reticulate pattern.

Dimensions: 53 (54.5) 56 μm; 2 specimens measured.

Comparison: *Diaphanospora milleri* Breuer and Steemans, 2013 is smaller and its sexine is randomly and finely folded. Its trilete mark is distinct.

Occurrence: JNDL-3 and JNDL-4; Hammamiyat and Murayr members; *lindlarensis–sextantii* Zone.

Genus ***Dibolisporites*** Richardson, 1965

Type species: *Dibolisporites echinaceus* (Eisenack) Richardson, 1965.

Dibolisporites* cf. *D. farraginis McGregor and Camfield, 1982 (Plate II, 13–18)

cf. 1982 *Dibolisporites farraginis* McGregor and Camfield: p. 38; pl. 8, Figs. 3–4; text-Fig. 54.

Description: Amb is sub-circular. Laesurae are straight, accompanied by labra, up to 1.5 μm wide each, extending to, or almost to, the equator. Exine is 1.0–1.5 μm thick. Proximo-equatorial and distal regions are sculptured with a heterogeneous mixture of spinae, coni, bacula and verrucae, 0.5–3.0 μm high, 0.5–3.0 μm wide at base, some of which may be locally fused at base. Sculptural elements are unevenly distributed. Contact areas are with similarly shaped but smaller and more widely scattered sculpture.

Dimensions: 45(58)70 μm; 13 specimens measured.

Remarks: Specimens assigned to this species could belong to a more or less intergrading series from those with predominantly conate and small verrucose sculpture (*D. farraginis* and *D. uncatus* (Naumova) McGregor and Camfield, 1982). McGregor and Playford (1992) define the *D. farraginis* Morphon. It includes sub-circular forms sculptured with a mixture of mostly discrete grana, coni, spinae, biform elements and verrucae of various sizes.

Comparison: *Dibolisporites farraginis* McGregor and Camfield, 1982 is very similar but has a thicker exine and might have slightly larger ornamentation.

Occurrence: JNDL-3 and JNDL-4; Hammamiyat Member; *lindlarensis–sextantii* Zone.

Genus ***Dictyotriletes*** Naumova, 1939 ex Ishchenko, 1952

Type species: *Dictyotriletes bireticulatus* (Ibrahim) Potonié and Kremp, 1955.

***Dictyotriletes* sp. 2** (Plate III, 1)

Description: Amb is sub-circular to sub-triangular. Laesurae are simple and extend to the patina. Exine is 2–3 μm thick equatorially. Exine is proximally thinner and laevigate. Proximo-equatorial and distal regions are bi-reticulate. Lumina of the larger mesh reticulum are polygonal and 3–6 μm in diameter. At muri junctions of this reticulum, flat-topped papillae occur and are 1–4 μm high. Lumina of the smaller mesh reticulum are sub-rounded and 0.5–2.5 μm Muri of both reticula are thin and low. Proximal region is laevigate.

Dimensions: 48 μm; 1 specimen measured.

Comparison: The bi-reticulum of *Dictyotriletes* sp. 2 is a unique feature among Devonian *Dictyotriletes* species.

Occurrence: JNDL-4; Subbat Member; *lindlarensis–sextantii* Zone.

Genus ***Emphanisporites*** McGregor, 1961

Type species: *Emphanisporites rotatus* McGregor emend. McGregor, 1973.

***Emphanisporites* sp. 2** (Plate III, 2–4)

Description: Amb is sub-circular. Laesurae are straight, simple, extending to, or almost to, the equator. Exine is 1–2 μm equatorially thick. Proximal radially arranged muri, 0.5–1.5 μm wide at equator are commonly fused to form a thick, darker zone in the middle of each contact area. Muri are numerous in each contact area, straight to slightly undulating, variable in width and do not reach the proximal pole. Distal surface is laevigate.

Dimensions: 23 (35) 38 μm; 3 specimens measured.

Occurrence: BAQA-1 and BAQA-2; Sha'iba and Subbat members; *papillensis–baqaensis* to *ovalis* zones.

Genus ***Insculptospora*** Marshall, 1985

Type species: *Inscultospora confossa* (Richardson) Marshall, 1985.

Insculptospora maxima sp. nov. (Plate III, 5–10; Plate IV, 1–2)

Holotype: JNDL-3 core hole, sample 389.0 ft, slide 68563, S30/4 (Plate IV, 1).

Paratype: JNDL-3 core hole, sample 374.0 ft, slide 68562, L44 (Plate III, 9).

Locus typicus and stratum typicum: JNDL-3 core hole, Hammamiyat Member of the Jauf Formation at Domat Al-Jandal, Saudi Arabia.

Derivation of name: Refers to the large size of the spore; from the Latin *maximus*, meaning the largest.

Diagnosis: A large laevigate *Insculptospora* species with nexine sculptured with grana to verrucae towards the proximal pole where the fusion of sculptural elements forms an irregular rugulate or reticulate pattern.

Description: Amb is circular to sub-circular. Laesurae are straight, simple and equal to seven-tenths to eight-tenths of the amb radius in length. Curvaturae are often barely visible. The two layers are closely appressed or show a variable separation, which is visible at the equatorial margin. Nexine is less than 1 μm thick, and always displays compression folds independent of sexine. Nexine is sculptured with grana to verrucae towards the proximal pole, where the fusion of sculptural elements forms an irregular rugulate or reticulate pattern. Sculptural elements are less than 2 μm wide. Sexine is single-layered, 1.5–3.0 μm thick and laevigate.

Dimensions: 82 (100) 128 μm; 27 specimens measured.

Comparison: *Inscultospora confossa* (Richardson) Marshall, 1985 is very similar in many aspects except that its sexine is strongly infrapunctate and can be double-layered.

Occurrence: JNDL-3; Hammamiyat Member; *lindlarensis-sextantii* Zone.

Genus ***Raistrickia*** Schopf et al. emend. Potonié and Kremp, 1954

Type species: *Raistrickia grovensis* Schopf et al., 1944.

***Raistrickia* sp. A** *in* Steemans (1989) (Plate IV, 3–5)

1989 *Raistrickia* sp. A; Steemans: p. 156; pl. 45, Fig. 17.

Description: Amb is sub-circular to sub-triangular. Laesurae are straight, simple and extending almost to the equator. Curvaturae are generally coincident with the equator in the interradial areas. Exine is 0.5–1 μm thick equatorially. Equatorial and distal regions are usually densely sculptured with small pila and bacula, sub-polygonal in plan view, up to 1.5 μm high and wide at base, rarely up to 2.5 μm at top, and 1 μm apart. The tops of elements are flat, slightly concave or irregular. Contact areas are granulate.

Dimensions: 31 (34) 39 μm; 3 specimens measured.

Comparison: *Verrucosisporites onustus* Breuer and Steemans, 2013 has also sculptural elements with expanded apices but these are larger.

Occurrence: JNDL-4; Subbat Member; *asymmetricus* Zone.

Genus ***Verruciretusispora*** Owens, 1971

Type species: *Verruciretusispora dubia* (Eisenack) Richardson and Rasul, 1978.

***Verruciretusispora* sp. 1** (Plate IV, 6–8)

Description: Amb is sub-circular. Laesurae are straight, simple or accompanied by labra, up to 2 μm in overall width, six-tenths to nine-tenths of the amb radius in length. Exine is 1–2 μm thick. Equatorial and distal regions are sculptured with verrucae, 1–2.5 μm wide, 0.5–1 μm high and 1–4 μm apart. Verrucae are sub-circular in plan view and rounded in profile. Contact areas are laevigate or granulate.

Dimensions: 55 (60) 70 μm; 3 specimens measured.

Occurrence: BAQA-1 and JNDL-4; Subbat Member; *milleri* to *asymmetricus* zones.

Genus ***Verrucosisporites*** Ibrahim emend. Smith, 1971

Type species: *Verrucosisporites verrucosus* (Ibrahim) Ibrahim, 1933.

***Verrucosisporites* sp. 2** (Plate IV, 9–13)

Description: Amb is sub-circular. Laesurae are straight, simple or accompanied by labra, up to 4 μm in overall width, half to three-fifths of

Plate III. Each figured specimen is identified by core hole, sample depth, slide number and England Finder Co-ordinate location. All figured specimens are at magnification ×1000 unless otherwise stated.

1. *Dictyotriletes* sp. 2. JNDL-4, 341.2 ft, 68671, S43/2.
2–4. *Emphanisporites* sp. 2.
2. BAQA-1, 346.8 ft, 66797, L50/4.
3. BAQA-2, 50.2 ft, 66812, Q50/3.
4. BAQA-1, 371.1 ft, 66801, R55/1.
5–10. *Insculptospora maxima* sp. nov.
5. JNDL-3, 353.8 ft, 68559, P39 (×750).
6. JNDL-3, 374.0 ft, 68562, T31 (×750).
7. JNDL-3, 389.0 ft, 68563, R27 (×750).
8. JNDL-3, 374.0 ft, 68562, V41/2 (×750).
9. Paratype, JNDL-3, 374.0 ft, 68562, L44 (×750).
10. JNDL-3, 374.0 ft, 68562, E41/2 (×750).

Plate IV. Each figured specimen is identified by core hole, sample depth, slide number and England Finder Co-ordinate location. All figured specimens are at magnification ×1000 (see on page 210).

1–2. *Insculptospora maxima* sp. nov.
1. Holotype, JNDL-3, 389.0 ft, 68563, S30/4.
2. JNDL-3, 389.0 ft, 68563, T26.
3–5. *Raistrickia* sp. A *in* Steemans (1989).
3. JNDL-4, 448.6 ft, 68693, E37.
4. JNDL-4, 499.1 ft, 68704, M30/2.
5. JNDL-4, 484.1 ft, 68699, M35.
6–8. *Verruciretusispora* sp. 1.
6. JNDL-4, 454.8 ft, 68694, W51/2.
7. BAQA-1, 308.3 ft, 66791, T40.
8. JNDL-4, 404.8 ft, 03CW258, U47.
9–13. *Verrucosisporites* sp. 2.
9. JNDL-4, 111.0 ft, 68608, V25.
10. JNDL-4, 120.0 ft, 68612, K57.
11. JNDL-3, 463.5 ft, 68578, S41.
12. JNDL-4, 160.7 ft, 68624, C46/3.
13. JNDL-4, 152.7 ft, 68622, T38.

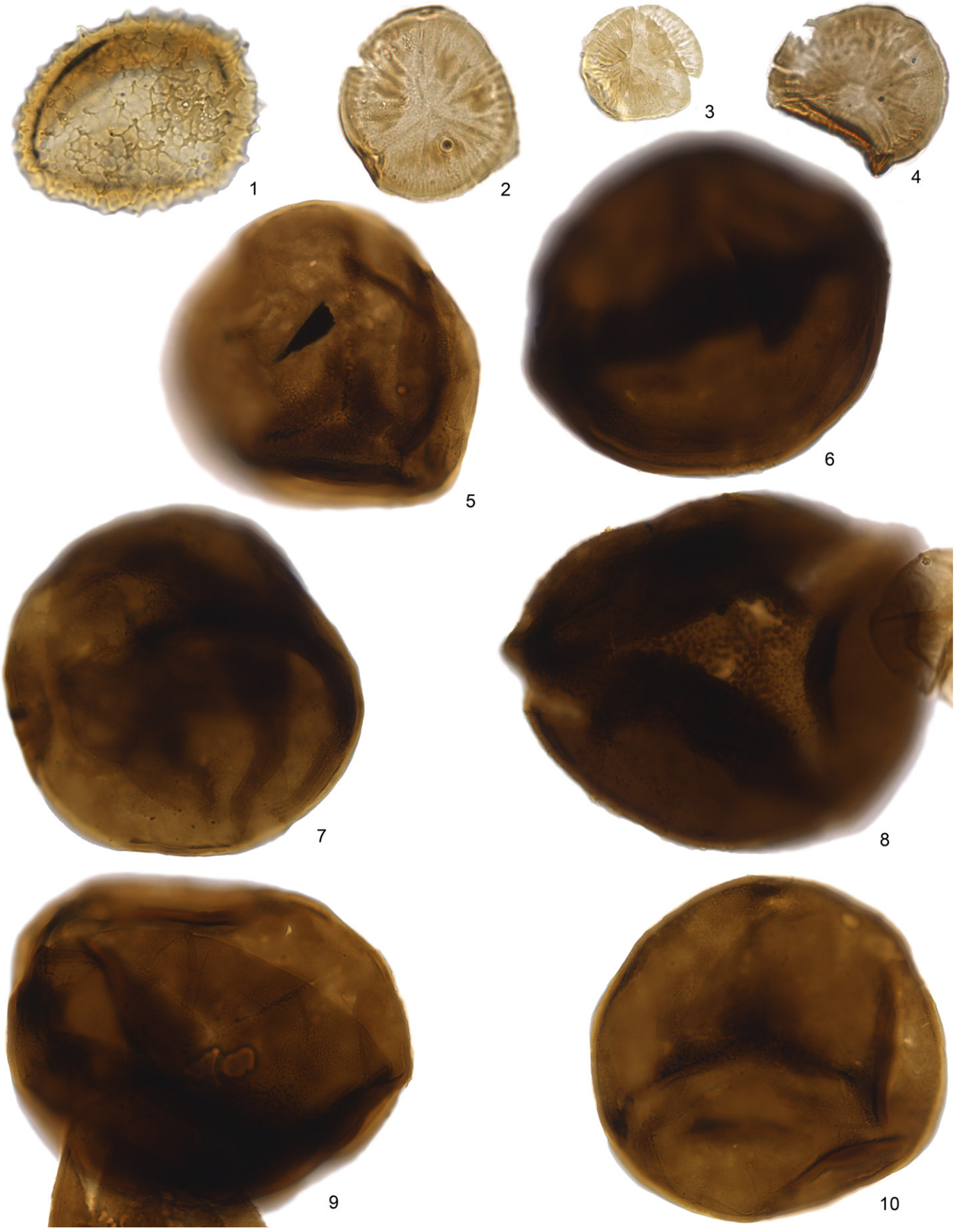
1
2
3
4
5
6
7
8
9
10

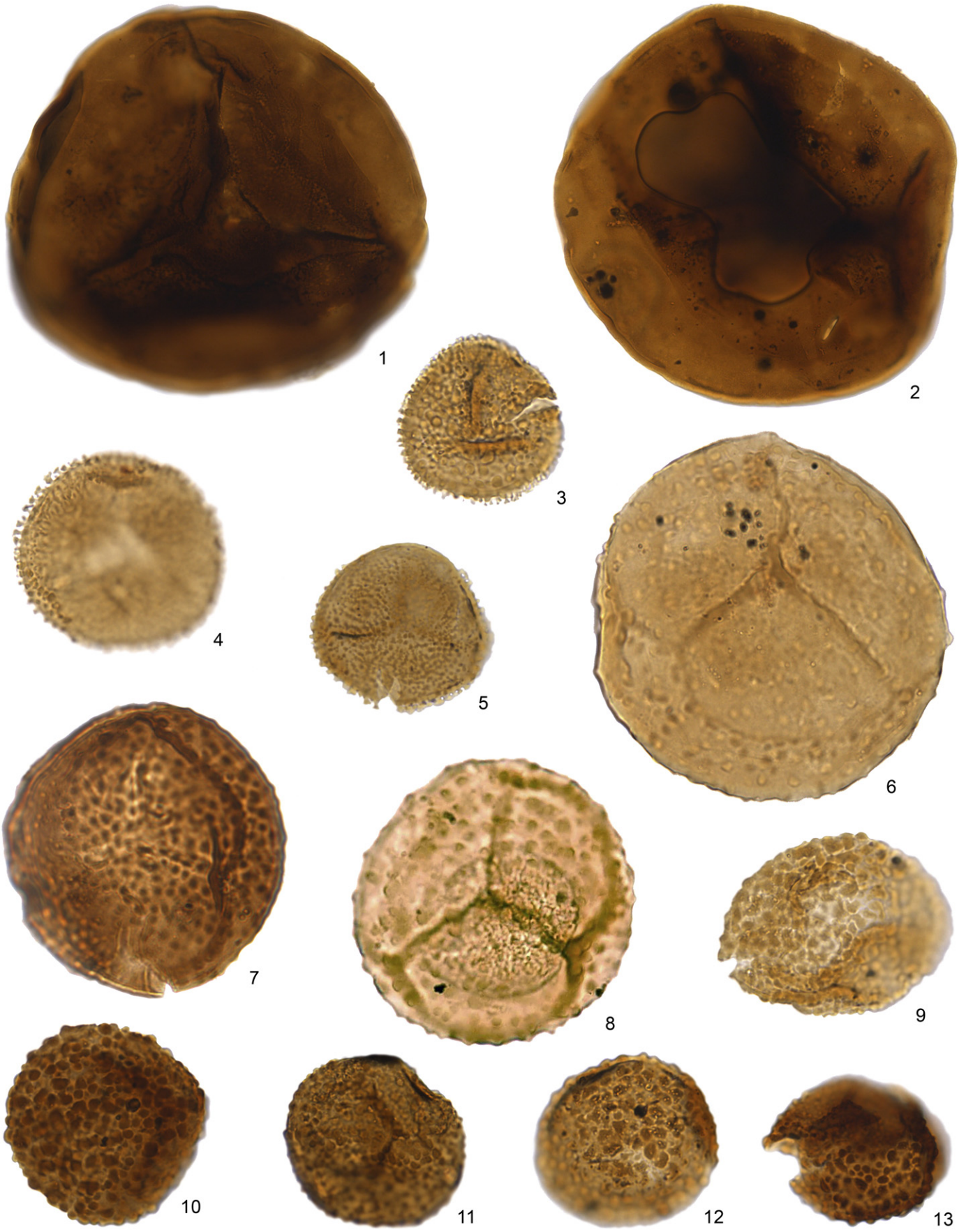

Plate IV. (*caption on page 208*)

the amb radius in length. Curvaturae are barely visible. Exine is c. 1 μm thick equatorially. Proximo-equatorial and distal regions are sculptured with variable verrucae commonly 0.5–3.0 μm wide at base, 0.5–1.0 μm high. Sculptural elements are rounded in profile, sub-polygonal to sub-rounded or irregular in plan view, and closely spaced. Proximal region laevigate or with reduced sculpture.

Dimensions: 35 (37) 44 μm; 5 specimens measured.

Comparison: *Verrucosisporites polygonalis* Lanninger, 1968 is larger and has a less variable ornamentation arranged in a polygonal pattern. Besides its verrucae can be flat-topped in profile.

Occurrence: JNDL-3 and JNDL-4; Hammamiyat Member; *lindlarensis–sextantii* Zone.

Appendix C. List of recorded spore taxa with full author citations

Acinosporites apiculatus (Streel) Streel, 1967
Acinosporites lindlarensis Riegel, 1968
Alatisporites trisacculus Breuer and Steemans, 2013
Ambitisporites asturicus (Rodriguez) Breuer and Steemans, 2013
Ambitisporites avitus Hoffmeister, 1959
Ambitisporites eslae (Cramer and Díez) Richardson et al., 2001
Amicosporites jonkeri (Riegel) Steemans, 1989
Amicosporites streelii Steemans, 1989
Aneurospora cf. *A. bollandensis* Steemans, 1989
Apiculiretusispora arabiensis Al-Ghazi, 2009
Apiculiretusispora brandtii Streel, 1964
Apiculiretusispora plicata (Allen) Streel, 1967
Archaeozonotriletes chulus (Cramer) Richardson and Lister, 1969
Artemopyra inconspicua Breuer et al., 2007
Artemopyra recticosta Breuer et al., 2007
Artemopyra? *scalariformis* Richardson, 1996
Biornatispora dubia (McGregor) Steemans, 1989
Biornatispora elegantula Breuer and Steemans, 2013
Biornatispora microclavata Breuer and Steemans, 2013
Breconisporites simplex Wellman 1993
Brochotriletes crameri Breuer and Steemans, 2013
Brochotriletes foveolatus Naumova, 1953
Brochotriletes hudsonii McGregor and Camfield, 1976
Brochotriletes robustus (Scott and Rouse) McGregor, 1973
Brochotriletes tenellus Breuer and Steemans, 2013
Camarozonotriletes alruwailii sp. nov.
Camarozonotriletes filatoffii Breuer et al., 2007
Camarozonotriletes retiformis (Hashemi and Playford) Breuer and Steemans, 2013
Camarozonotriletes sextantii McGregor and Camfield, 1976
Chelinospora carnosa Breuer and Steemans, 2013
Chelinospora condensata Breuer and Steemans, 2013
Chelinospora densa Breuer and Steemans, 2013
Chelinospora laxa Breuer and Steemans, 2013
Chelinospora retorrida Turnau, 1986
Chelinospora vulgata Breuer and Steemans, 2013
Cirratriradites? *diaphanus* Steemans, 1989
Clivosispora verrucata McGregor, 1973 var. *convoluta* McGregor and Camfield, 1976
Clivosispora verrucata McGregor, 1973 var. *verrucata* McGregor and Camfield, 1976
Concentricosisporites sagittarius (Rodriguez) Rodriguez, 1983
Coronaspora inornata Breuer and Steemans, 2013
Cymbohilates baqaensis Breuer et al., 2007
Cymbohilates comptulus Breuer et al., 2007
Cymbohilates cymosus Richardson, 1996
Cymbohilates heteroverrucosus Breuer et al., 2007
Cymbosporites asymmetricus Breuer et al., 2007
Cymbosporites dammamensis Steemans, 1995
Cymbosporites dittonensis Richardson and Lister, 1969
Cymbosporites echinatus Richardson and Lister, 1969
Cymbosporites paulus McGregor and Camfield, 1976
Cymbosporites rarispinosus Steemans, 1989
Cymbosporites senex McGregor and Camfield, 1976
Cymbosporites stellospinosus Steemans, 1989 var. *minor* Breuer and Steemans, 2013
Cymbosporites variabilis var. *densus* Breuer and Steemans, 2013
Cymbosporites variabilis var. *dispersus* Breuer and Steemans, 2013
Cymbosporites variabilis var. *variabilis* Breuer and Steemans, 2013
Cymbosporites wellmanii Breuer and Steemans, 2013
Devonomonoletes crassus sp. nov.
Devonomonoletes sp. 1 *in* Breuer and Steemans, 2013
Diaphanospora milleri Breuer and Steemans, 2013
?*Diaphanospora* sp. 1
Diatomozonotriletes franklinii McGregor and Camfield, 1982
Dibolisporites bullatus (Allen) Riegel, 1973
Dibolisporites echinaceus (Eisenack) Richardson, 1965 sensu stricto
Dibolisporites eifeliensis (Lanninger) McGregor, 1973
Dibolisporites cf. *D. farraginis* McGregor and Camfield, 1982
Dibolisporites gaspiensis (McGregor) Breuer and Steemans, 2013
Dibolisporites tuberculatus Breuer and Steemans, 2013
Dibolisporites verecundus Breuer and Steemans, 2013
Dibolisporites sp. 1 *in* Breuer and Steemans (2013)
Dibolisporites sp. 2 *in* Breuer and Steemans (2013)
Dictyotriletes biornatus Breuer et al., 2007 var. *biornatus* Breuer and Steemans, 2013
Dictyotriletes biornatus Breuer et al., 2007 var. *murinatus* Breuer and Steemans, 2013
Dictyotriletes emsiensis (Allen) McGregor, 1973
Dictyotriletes favosus McGregor and Camfield, 1976
Dictyotriletes ?*gorgoneus* Cramer, 1966a *in* McGregor (1973)
Dictyotriletes granulatus Steemans, 1989
Dictyotriletes marshallii Breuer and Steemans, 2013
Dictyotriletes subgranifer McGregor, 1973
Dictyotriletes sp. 1 *in* Breuer and Steemans, 2013
Dictyotriletes sp. 2
Dyadaspora murusattenuata Strother and Traverse, 1979
Emphanisporites annulatus McGregor, 1961
Emphanisporites cf. *E. biradiatus* Steemans, 1989
Emphanisporites decoratus Allen, 1965
Emphanisporites cf. *E. edwardsiae* Wellman, 2006
Emphanisporites erraticus (Eisenack) McGregor, 1961
Emphanisporites mcgregorii Cramer, 1966a
Emphanisporites plicatus Breuer and Steemans, 2013
Emphanisporites rotatus McGregor emend. McGregor, 1973
Emphanisporites schultzii McGregor, 1973
Emphanisporites sp. 2
Gneudnaspora divellomedia (Chibrikova) Balme, 1988 var. *divellomedia* Breuer et al., 2007
Gneudnaspora divellomedia (Chibrikova) Balme, 1988 var. *minor* Breuer et al., 2007
Grandispora protea (Naumova) Moreau-Benoit, 1980b
Granulatisporites concavus Breuer and Steemans, 2013
Iberoespora cantabrica Cramer and Díez, 1975
Iberoespora glabella Cramer and Díez, 1975
Iberoespora cf. *I. guzmani* Cramer and Díez, 1975
Insculptospora maxima sp. nov.
?*Knoxisporites riondae* Cramer and Díez, 1975
Latosporites ovalis Breuer et al., 2007
Leiozosterospora cf. *L. andersonii* Wellman, 2006
Lycospora culpa Allen, 1965
Perotrilites caperatus (McGregor) Steemans, 1989
Raistrikia jaufensis Breuer and Steemans, 2013
Raistrickia sp. A *in* Steemans (1989)
Reticuloidosporites antarcticus Kemp, 1972
Retusotriletes atratus Breuer and Steemans, 2013
Retusotriletes celatus Breuer and Steemans, 2013

Retusotriletes goensis Lele and Streel, 1969
Retusotriletes maculatus McGregor and Camfield, 1976
Retusotriletes rotundus (Streel) Streel emend. Lele and Streel, 1969
Retusotriletes tenerimedium Chibrikova, 1959
Retusotriletes triangulatus (Streel) Streel, 1967
Rhabdosporites minutus Tiwari and Schaarschmidt, 1975
Scylaspora costulosa Breuer et al., 2007
Stellatispora multicostata Breuer et al., 2007
Synorisporites papillensis McGregor, 1973
Tetrahedraletes medinensis Strother and Traverse emend. Wellman and Richardson, 1993
Verruciretusispora dubia (Eisenack) Richardson and Rasul, 1978
Verruciretusispora sp. 1
Verrucosisporites nafudensis Breuer and Steemans, 2013
Verrucosisporites onustus Breuer et al., 2007
Verrucosisporites polygonalis Lanninger, 1968
Verrucosisporites stictus Breuer and Steemans, 2013
Verrucosisporites sp. 1 *in* Breuer and Steemans (2013)
Verrucosisporites sp. 2
Zonohilates vulneratus gen. et sp. nov.
Zonotriletes brevivelatus Breuer and Steemans, 2013
Zonotriletes rotundus Breuer and Steemans, 2013
Zonotriletes venatus Breuer and Steemans, 2013

References

Al-Ghazi, A., 2007. New evidence for the Early Devonian age of the Jauf Formation in northern Saudi Arabia. In: Paris, F., Owens, B., Miller, M.A. (Eds.), Palaeozoic Palynology of the Arabian Plate and Adjacent Areas. Revue de Micropaléontologie 50, pp. 59–72.

Al-Hajri, S.A., Owens, B., 2000. Stratigraphic Palynology of the Palaeozoic of Saudi Arabia. GeoArabia Special Publication 1. Gulf PetroLink, Bahrain (231 pp.).

Al-Hajri, S.A., Filatoff, J., Wender, L.E., Norton, A.K., 1999. Stratigraphy and operational palynology of the Devonian System in Saudi Arabia. GeoArabia 4 (1), 53–68.

Al-Husseini, M.I., Matthews, R.K., 2005. Arabian orbital stratigraphy: second-order sequence boundaries? GeoArabia 10 (2), 165–184.

Al-Husseini, M.I., Matthews, R.K., 2006. Devonian Jauf Formation, Saudi Arabia: orbital second-order Depositional Sequence 28. GeoArabia 11 (2), 53–70.

Al-Laboun, A.A., 1982. The subsurface stratigraphy of the pre-Khuff formations in central and northwestern Arabia(Ph.D. Thesis) Faculty of Earth Sciences. King Abdulaziz University, Jeddah, Saudi Arabia.

Al-Laboun, A.A., 1986. Stratigraphy and hydrocarbon potential of the Paleozoic succession in both Tabuk and Widyan basins, Arabia. In: Halbouty, M.L. (Ed.), Future Petroleum Provinces of the World. Memoir of the American Association of Petroleum Geologists 40, pp. 373–397.

Allen, K.C., 1965. Lower to Middle Devonian spores of North and Central Vestspitsbergen. Palaeontology 8, 687–748.

Arkhangelskaya, A.D., 1985. Zonal spore assemblages and stratigraphy of the Lower and Middle Devonian in the Russian Plate. In: Menner, V.V., Byvsheva, T.V. (Eds.), Atlas of Spores and Pollen from the Phanerozoic Petroleum Formations in the Russian and Turanian Plates. Trudy Vsesoiuznogo Nauchno-Issledovatel'skogo Geologorazve-dochnogo Neftianogo institute (VNIGNI) 253, pp. 5–21 (in Russian).

Bahafzallah, A., Jux, U., Omara, S., 1981. Stratigraphy and facies of the Devonian Jauf Formation, Saudi Arabia. N. Jb. Geol. Paläont. (Monatsh.) 1, 1–18.

Balme, B.E., Hassell, C.W., 1962. Upper Devonian spores from the Canning Basin, Western Australia. Micropaleontology 8, 1–28.

Boucot, A.J., McClure, H.A., Alvarez, F., Ross, J.R.P., Taylor, D.W., Struve, W., Savage, N.N., Turner, S., 1989. New Devonian fossils from Saudi Arabia and their biogeographical affinities. Senckenb. Lethaea 69, 535–597.

Breuer, P., 2007. Devonian miospore palynology in Western Gondwana: an application to oil exploration(Ph.D. Thesis) University of Liège, Liège, Belgium.

Breuer, P., Steemans, P., 2013. Devonian spore assemblages from northwestern Gondwana: taxonomy and biostratigraphy. Spec. Pap. Palaeontol. 89, 1–163.

Breuer, P., Al-Ghazi, A., Filatoff, J., Higgs, K.T., Steemans, P., Wellman, C.H., 2005. Stratigraphic palynology of Devonian boreholes from northern Saudi Arabia. In: Steemans, P., Javaux, E. (Eds.), Pre-Cambrian to Palaeozoic Palaeopalynology and Palaeobotany. Carnets de Géologie / Notebooks on Geology, Memoir 2005/02, Abstract 01.

Breuer, P., Al-Ghazi, A., Al-Ruwaili, M., Higgs, K.T., Steemans, P., Wellman, C.H., 2007. Early to Middle Devonian miospores from northern Saudi Arabia. In: Paris, F., Owens, B., Miller, M.A. (Eds.), Palaeozoic Palynology of the Arabian Plate and Adjacent Areas. Revue de Micropaléontologie 50, pp. 27–57.

Burgess, N.D., Richardson, J.B., 1991. Silurian cryptospores and spores from the type Wenlock area, Shropshire, England. Palaeontology 34, 601–628.

Forey, P.L., Young, V.T., McClure, H.A., 1992. Lower Devonian fishes from Saudi Arabia. Bull. Br. Mus. Nat. Hist. (Geol.) 48 (2), 25–43.

Gerrienne, P., Bergamaschi, S., Pereira, E., Rodrigues, M.A.C., Steemans, P., 2001. An Early Devonian flora, including *Cooksonia* from the Paraná Basin (Brazil). In: Gerrienne, P. (Ed.), Early land plants evolution and diversification. Review of Palaeobotany and Palynology 116, pp. 19–38.

Grahn, Y., 2005. Devonian chitinozoan biozones of Western Gondwana. Acta Geol. Pol. 55 (3), 211–227.

Grahn, Y., Mendlowicz Mauller, P., Breuer, P., Pinto Bosetti, E.P., Bergamaschi, S., Pereira, E. , 2010. The Furnas/Ponta Grossa contact and the age of the lowermost Ponta Grossa Formation in the Apucarana Sub-basin (Paraná Basin, Brazil): integrated palynological age determination. Rev. Bras. Paleontol. 13 (2), 89–102.

Grignani, D., Lanzoni, E., Elatrash, H., 1991. Palaeozoic and Mesozoic subsurface palynostratigraphy in the Al Khufrah Basin, Libya. In: Salem, M.J., Hammuda, O.S., Eliagoubi, B.A. (Eds.), The Geology of Libya (Third Symposium on the Geology of Libya, Tripoli, 27–30 September 1987) 4. Elsevier, Amsterdam, pp. 1159–1227.

Helal, A.H., 1965. General geology and lithostratigraphic subdivision of the Devonian rocks of the Jauf area, Saudi Arabia. N. Jb. Geol. Paläont. (Monatsh.) 9, 527–551.

Ibrahim, A.C., 1933. Sporenformen des Ägirhorizontes des Ruhrreviers(Dissertation) Technische Hoschschule Berlin.

Ishchenko, A.M., 1952. Atlas of the microspores and pollen of the Middle Carboniferous of the western part of the Donetz Basin. Akademiya Nauk Ukrainskoy SSR. Trudy Instituta Geologischeskikh Nauk, pp. 1–83 (in Russian).

Janjou, D., Halawani, M.A., Al-Muallem, M.S., Robelin, C., Brosse, J.-M., Courbouleix, S., Dagain, J., Genna, A., Razin, P., Roobol, J.M., Shorbaji, H., Wyns R., 1997a. Explanatory notes to the geologic map of the Al Qalibah Quadrangle, Kingdom of Saudi Arabia. Geoscience Map GM-135, scale 1:250,000, sheet 28C. Deputy Ministry for Mineral Resources, Ministry of Petroleum and Mineral Resources, Kingdom of Saudi Arabia. 44 p.

Janjou, D., Halawani, M.A., Brosse, J.-M., Al-Muallem, M.S., Becq-Giraudon, J.F., Dagain, J., Genna, A., Razin, P., Roobol, M.J., Shorbaji, H., Wyns, R., 1997b. Explanatory notes to the geologic map of the Tabuk Quadrangle, Kingdom of Saudi Arabia. Geoscience Map GM-137, scale 1:250,000, sheet 28B. Deputy Ministry for Mineral Resources, Ministry of Petroleum and Mineral Resources, Kingdom of Saudi Arabia. 49 p.

Konert, G., Al-Afifi, A.M., Al-Hajri, S.A., Droste, H.J., 2001. Paleozoic stratigraphy and hydrocarbon habitat of the Arabian Plate. GeoArabia 6 (3), 407–442.

Lanninger, E.P., 1968. Sporen-Gesellschaften aus dem Ems der SW-Eifel (Rheinisches Schiefergebirge). Palaeontogr. Abt. B 122, 95–170.

Lebret, P., Halawani, M.A., Memesh, A., Bourdillon, C., Janjou, D., Le Nindre, Y.-M., Roger, J., Shorbaji, H., Kurdi, H., 1999. Explanatory notes to the geologic map of the Turubah Quadrangle, Kingdom of Saudi Arabia. Geoscience Map GM-139, scale 1:250,000, sheet 28 F. Deputy Ministry for Mineral Resources, Ministry of Petroleum and Mineral Resources, Kingdom of Saudi Arabia. 46 p.

Lelièvre, H., Janvier, P., Janjou, D., Halawani, M.A., 1995. *Nefudina qalibahensis* nov. gen., nov. sp. un rhénanide (Vertebrata, Placodermi) du Dévonien Inférieur de la Formation de Jauf (Emsien) d'Arabie Saoudite. Geobios 19, 109–115.

Leszczyński, S., Breuer, P., Miller, M.A., 2010. Ichnology of the Early Devonian Jauf Formation in northern Saudi Arabia. GEO 2010, Manama (Bahrain), March 7–10, 2010.

Loboziak, S., Streel, M., 1995. Late Lower and Middle Devonian miospores from Saudi Arabia. Rev. Palaeobot. Palynol. 89, 105–113.

Lozej, G.P., 1983. Geological and geochemical reconnaissance exploration of the cover rocks in northwestern Hijaz. Open-file report RF-OF-03-2. Deputy Ministry for Mineral Resources, Jeddah, Saudi Arabia.

Marshall, J.E.A., 1985. *Insculptospora*, a new genus of Devonian camerate spore with a sculptured intexine. Pollen Spores 27, 453–470.

McGregor, D.C., 1961. Spores with proximal radial pattern from the Devonian of Canada. Bull. Geol. Surv. Can. 76, 1–11.

McGregor, D.C., 1973. Lower and Middle Devonian spores of Eastern Gaspé, Canada. I. Systematics. Palaeontogr. Abt. B 142, 1–77.

McGregor, D.C., Camfield, M., 1976. Upper Silurian? to Middle Devonian spores of the Moose River Basin, Ontario. Bull. Geol. Surv. Can. 263, 1–63.

McGregor, D.C., Camfield, M., 1982. Middle Devonian spore from the Cape De Bray, Weatherall, and Hecla Bay Formations of northeastern Melville Island, Canadian Artic. Bull. Geol. Surv. Can. 348, 1–105.

McGregor, D.C., Playford, G., 1992. Canadian and Australian Devonian spores: zonation and correlation. Bull. Geol. Surv. Can. 438, 1–125.

Melo, J.H.G., Loboziak, S., 2003. Devonian–Early Carboniferous miospore biostratigraphy of the Amazon Basin, Northern Brazil. Rev. Palaeobot. Palynol. 124, 131–202.

Mendlowicz Mauller, P., Machado Cardoso, T.R., Pereira, E., Steemans, P., 2007. Resultados Palinoestratigráficos do Devoniano da Sub-Bacia de Alto Garças (Bacia do Paraná—Brasil). In: Carvalho, I.S., Cassab, R.C.T., Schwanke, C., Carvalho, M.A., Fernandes, A.C.S., Rodrigues, M.A.C., Carvalho, M.S.S., Arai, M., Oliveira, M.E.Q. (Eds.), Paleontologia: cenários de Vida 1. Interciência, Rio de Janeiro, pp. 607–619.

Naumova, S.N., 1939. Spores and pollen of the coals of the USSR. 17th International Geological Congress, Report 1. Moscow, Russia, pp. 353–364 (In Russian).

Naumova, S.N., 1953. Spore–pollen assemblages of the Upper Devonian of the Russian Platform and their stratigraphic value. Akademiya Nauk SSSR, Institut Geologii Nauk, 143. Geological Series 60 (203 pp. (in Russian)).

Owens, B., 1971. Spores from the Middle and Early Upper Devonian rocks of the Western Queen Elizabeth Island, Arctic Archipelago. Pap. Geol. Surv. Can. 70–38, 1–157.

Potonié, R., Kremp, G.O.W., 1954. Die Gattungen der paläozoischen Sporae dispersae und ihre Stratigraphie. Geol. Jahrb. 69, 111–194.

Potonié, R., Kremp, G.O.W., 1955. Die Sporae dispersae des Ruhrkarbons. Ihre Morphographie und Stratigraphie mit Ausblicken auf Arten anderer Gebiete und Zeitabschnitte. Teil I. Palaeontogr. Abt. B 98, 1–136.

Powers, R.W., 1968. Asie: Arabie Saoudite. Lexique Stratigraphique Internationale. Edition du CNRS, Paris (177 pp.).

Rahmani, R.A., 2004. Facies and sequences of Devonian Jauf Reservoir, Ghawar Field, Saudi Arabia. 6th Middle East Geosciences Conference, GEO 2004. GeoArabia, Abstract 9(1), p. 118.

Rahmani, R.A., Steel, R.J., Al-Duaiji, A.A., 2002. High-resolution sequence stratigraphy of the Devonian Jauf gas reservoir: a shoreface and estuarine embayment succession, greater Ghawar area, eastern Saudi Arabia. 5th Middle East Geosciences Conference, GEO 2002. GeoArabia, Abstract 7(2), p. 288.
Richardson, J.B., 1965. Middle Old Red Sandstone spore assemblages from the Orcadian Basin north-east Scotland. Palaeontology 7, 559–605.
Richardson, J.B., 1996. Taxonomy and classification of some new Early Devonian cryptospores from England. In: Cleal, C.J. (Ed.), Studies on early land–plant spores from Britain. Special Papers in Palaeontology 55, pp. 7–40.
Richardson, J.B., McGregor, D.C., 1986. Silurian and Devonian spore zones of the Old Red Sandstone Continent and adjacent regions. Bull. Geol. Surv. Can. 364, 1–179.
Richardson, J.B., Rasul, S.M., 1978. Palynomorphs in Lower Devonian sediments from the Apley Barn Borehole, southern England. Pollen Spores 20, 423–462.
Riegel, W., 1982. Palynological aspects of the Lower/Middle Devonian transition in the Eifel Region. Cour. Forsch.-Inst. Senckenberg 55, 279–292.
Rubinstein, C.V., Melo, J.H.G., Steemans, P., 2005. Lochkovian (earliest Devonian) miospores from the Solimões Basin, northern Brazil. Rev. Palaeobot. Palynol. 133, 91–113.
Schopf, J.M., Wilson, L.R., Bentall, R., 1944. An annotated synopsis of Paleozoic fossil spores and the definition of generic groups. Illinois State Geological Survey, Report of Investigations 91, pp. 1–66.
Scotese, C.R., 2000. Atlas of Earth History. PALEOMAP Project, (52 pp. Arlington. http://www.scotese.com/earth.html).
Sharland, P.R., Archer, R., Casey, D.M., Davies, R.B., Hall, S.H., Heward, A.P., Horbury, A.D., Simmons, M.D. (Eds.), 2001. Arabian Plate Sequence StratigraphyGeoArabia. Gulf PetroLink, Bahrain (371 p. and 3 enclosures).
Smith, A.H.V., 1971. Le genre *Verrucosisporites* Ibrahim 1933 emend. Microfossiles organiques du Paléozoïque. Commission Internationale de Microflore du Paléozoïque, Spores 4, pp. 35–87.
Steemans, P., 1989. Palynostratigraphie de l'Eodévonien dans l'ouest de l'Europe. Service Géologique de Belgique, Mémoires pour servir à l'Explication des Cartes Géologiques et Minières de la Belgique 27, pp. 1–453.
Steemans, P., 1995. Silurian and Lower Emsian spores in Saudi Arabia. Rev. Palaeobot. Palynol. 89, 91–104.
Steemans, P., Rubinstein, C., Melo, J.H.G., 2008. Siluro-Devonian miospore biostratigraphy of the Urubu River area, western Amazon Basin, northern Brazil. Geobios 41, 263–282.
Streel, M., 1965. Techniques de préparation des roches détritiques en vue de l'analyse palynologique quantitative. Ann. Soc. Geol. Belg. 88, 107–117.
Streel, M., Higgs, K.T., Loboziak, S., Riegel, W., Steemans, P., 1987. Spore stratigraphy and correlation with faunas and floras in the type marine Devonian of the Ardenne-Rhenish region. Rev. Palaeobot. Palynol. 50, 211–219.
Streel, M., Loboziak, S., Steemans, P., Bultynck, P., 2000. Devonian miospore stratigraphy and correlation with the global stratotype sections and points. In: Bultynck, P. (Ed.), Subcommission on Devonian Stratigraphy. Fossil Groups Important for Boundary Definition. Courier Forschungsinstitut Senckenberg 220, pp. 9–23.
Strother, P.K., 1994. Sedimentation of palynomorphs in rocks of pre-Devonian age. In: Traverse, A. (Ed.), Sedimentation of Organic Particles. Cambridge University Press, Cambridge, pp. 489–502.
Traverse, A., 2007. 2nd edition. Paleopalynology 28. Springer, (814 pp.).
Troth, I., Marshall, J.E.A., Racey, A., Becker, R.T., 2011. Devonian sea-level change in Bolivia: a high palaeolatitude biostratigraphical calibration of the global sea-level curve. Palaeogeogr. Palaeoclimatol. Palaeoecol. 304, 3–20.
Vaslet, D., Kellogg, K.S., Berthiaux, A., Le Strat, P., Vincent, P.-L., 1987. Explanatory notes to the geologic map of the Baq'a Quadrangle, Kingdom of Saudi Arabia. Geoscience Map GM-116 C, scale 1:250,000, sheet 27 F. Deputy Ministry for Mineral Resources, Ministry of Petroleum and Mineral Resources, Kingdom of Saudi Arabia. 45 p.
Wallace, C.A., Dini, S.M., Al-Farasani, A.A., 1996. Explanatory notes to the geological map of the Ash Shuwahitiyah Quadrangle, Kingdom of Saudi Arabia. Geoscience Map GM-125C, scale 1:250,000, sheet 30D. Deputy Ministry for Mineral Resources, Ministry of Petroleum and Mineral Resources, Kingdom of Saudi Arabia. 27 p.
Wallace, C.A., Dini, S.M., Al-Farasani A.A., 1997. Explanatory notes to the geological map of the Al Jawf Quadrangle, Kingdom of Saudi Arabia. Geoscience Map GM-128C, scale 1: 250,000, sheet 29D. Deputy Ministry for Mineral Resources, Ministry of Petroleum and Mineral Resources, Kingdom of Saudi Arabia. 31 p.
Wender, L.E., Bryant, J.W., Dickens, M.F., Neville, A.S., Al-Moqbel, A.M., 1998. Paleozoic (pre-Khuff) hydrocarbon geology of the Ghawar area, eastern Saudi Arabia. GeoArabia 3 (2), 273–302.
Ziegler, W., 2000. The Lower Eifelian Boundary. Cour. Forsch.-Inst. Senckenberg 225, 27–36.